LUND UNIVERSITY

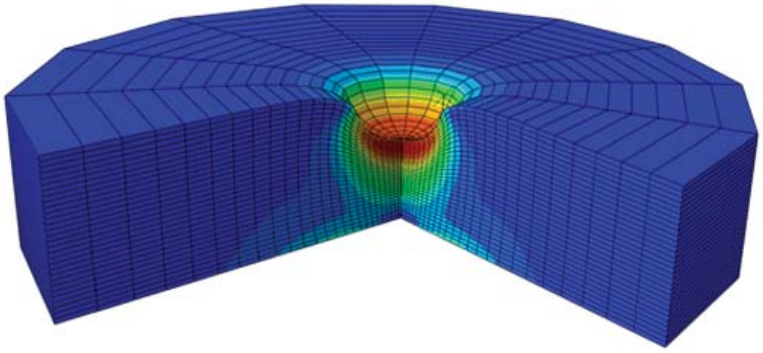

STATIC AND DYNAMIC CHARACTERIZATION OF ELASTOMERS BY A MODIFIED HARDNESS TEST

OMAR CHOUMAN

Structural Mechanics

Master's Dissertation

DEPARTMENT OF CONSTRUCTION SCIENCES
DIVISION OF STRUCTURAL MECHANICS

ISRN LUTVDG/TVSM--19/5237--SE (1-71) | ISSN 0281-6679
MASTER'S DISSERTATION

STATIC AND DYNAMIC CHARACTERIZATION OF ELASTOMERS BY A MODIFIED HARDNESS TEST

OMAR CHOUMAN

Supervisor: Professor **PER-ERIK AUSTRELL**, Division of Structural Mechanics, LTH.
Examiner: Professor **KENT PERSSON**, Division of Structural Mechanics, LTH.

Printed by V-husets tryckeri LTH, Lund, Sweden, October 2019 *(Pl)*.

For information, address:
Division of Structural Mechanics,
Faculty of Engineering LTH, Lund University, Box 118, SE-221 00 Lund, Sweden.
Homepage: www.byggmek.lth.se

Foreword

This master's thesis covers 30 credits and was carried out as a joint project at the Division of Structural Mechanics at the Faculty of Engineering, Lund University and at Volvo Cars in Gothenburg.

I would like to thank my supervisor Per-Erik Austrell for all the input and guidance that I received during the work. I would also like to thank Volvo Cars, especially Kai Kallio and Johan Samuelsson, for inviting me to their test labs in Gothenburg and showing me how the different experimental tests are performed for rubber materials. Finally, I would like to thank Lund University and Lunarc for giving me access to Aurora and all the software's included that were used in this work.

Lund
August 2019

Omar Chouman

Abstract

Today rubber can be found in many different applications, such as vibration dampers, tyres, clothes and gaskets. Two different types of rubbers are used today, namely the natural rubber and synthetic rubber. Natural rubber is made of a milky substance called latex, which is obtained from special trees found in tropical countries. Synthetic rubber is also made from latex, but the latex is obtained in labs by combining different chemicals together. Different fillers can also be added in order to change the properties of both natural and synthetic rubber, resulting in over 1000 different rubber materials with different characteristics and behaviours.

A standard hardness test is always done on rubber which classifies the hardness of the rubber and is measured in either a Shore scale or IRHD scale.

The static and dynamic material parameters, which are used in finite element simulations, are traditionally characterised using experimental methods which relies on homogenous stress states. Simple shear test is most commonly used when both static and dynamic characterizations are done, but in practice it is hard to obtain homogenous stress state because of several different factors. The static material parameters are obtained by fitting a hyperelastic material model, such as the Yeoh model, with the response (stresses and strains) obtained from experimental tests. The dynamic parameters are obtained by fitting experimental data, such as dynamic shear modulus G_{dyn} and damping d, with viscoelastic-elastoplastic material models using a minimization approach.

An alternative method has been evaluated in this project, where the standard hardness test is modified into doing a displacement-controlled loading with the indentation force being measured for a fixed number of indentation depths. The material parameters are then obtained by using an energy balance equation, which contains:

- the response (force and displacement) measured from the experiments,
- the state of deformation obtained from finite element method and
- the unknown material parameters (hyperelastic constants for static analysis, G_{dyn} and d for dynamic analysis).

When it comes to the static analysis of the modified hardness test it has shown to be a very good method in a work done by Austrell [5], where three natural rubbers with different hardness values where evaluated using the finite element method.

The dynamic analysis has been evaluated in this thesis, and three synthetic rubbers with different responses were used. The goal is to be able to find the dynamic shear modulus $G_{dyn}(\kappa_{eq}, f)$ and damping $d(\kappa_{eq}, f)$ which are similar to the ones obtained from simple shear test in order to use the same fitting procedure when obtaining the viscoelastic-elastoplastic material parameters.

The damping is calculated the same way as for simple shear test and should not be a problem to calculate since it is insensitive to the boundary condition. The problem is to find a connection between the indentation amplitude u_{dyn} and the shear amplitude κ_{dyn}, and what was done in

this project was that pure compression was assumed for the modified hardness test, and the strain invariants for compression and shear were put equal to each other resulting in the following approximative connection

$$u_{shear} = \sqrt{3} \cdot u_{compression}$$

The basis of the dynamic analysis is the same energy balance as for the static analysis, but with a slight modification in order to connect the tangential modulus K_{dyn} from the modified hardness test with the dynamic shear modulus G_{dyn} from the simple shear test. Only the most influenced elements were used in the energy balance equation, but the results obtained from this method were not good at all. Dynamic shear modulus did not show any dependence of the frequency nor the amplitude, and it also varied between the different types of materials. Therefore another approach was tested, where K_{dyn} was compared directly with G_{dyn} by assuming a linear connection

$$\alpha \cdot K_{dyn} = G_{dyn}$$

This method showed to be very good since a single value of alpha was obtained for the different rubber materials, and the frequency and amplitude dependence where almost spot on compared to the simple shear test when the amplitude connection $u_{shear} = \sqrt{3} \cdot u_{comp}$ was used.

The damping obtained from the modified hardness test showed a similar behaviour as for the simple shear test when it comes to the frequency dependence, but there was a slight difference in amplitude dependence, this when both the same amplitudes were used, and when the amplitude connection $u_{shear} = \sqrt{3} \cdot u_{comp}$ was used.

List of contents

1 Introduction

1.1 Background

The traditional method of material testing and parameter identification is based on a homogenous stress state. In order to achieve this different types of material testing's are performed, for example simple shear test and lubricated compression test. In practice it is hard to achieve homogenous state and it is also expensive since special testing specimens must be manufactured. Therefore a simpler method, which relies on inhomogeneous state, is going to be investigated experimentally, theoretically and by finite element method, namely the modified hardness test.

The FEM part aims at obtaining static and dynamic material parameters for two rubber specimens, one using the modified hardness test and the other using a double shear specimen as a reference. For quasi static loading the Yeoh constants, which are hyper elastic parameters, will be determined and compared between the two different specimens. For the dynamic harmonic loading the dynamic shear modulus and damping are extracted from the two specimens and compared. The goal is to find the dynamic shear modulus G_{dyn} and damping d as a function of amplitude and frequency in a simpler and faster way.

The basis for the method is going to be an energy balance equation (external work = stored strain energy). The quasi static part has already been evaluated theoretically by Austrell [5], and the investigation was done using finite element simulations which was working quite well, but it needs to be verified by physical testing. However, the dynamic part has not been evaluated thoroughly which will be done in this project using the finite element method.

1.2 Objective

The aim is to simplify the material characterization of rubber materials, where the dynamic and static material parameters are to be used in FE-simulations.

1.3 Method

To evaluate the simplified method a literature study is initiated in order to gather information regarding the behavior of rubber materials and how it is modelled using the finite element method. Thereafter the traditional material testing (simple shear test) and the modified hardness test are performed on different rubbers and the dynamic shear modulus and damping are extracted and compared. The tests are performed in ABAQUS, and the results are evaluated using MATLAB.

1.4 Limitations

The analysis in this thesis is focused on the dynamic characterization of material parameters, since it has not been evaluated yet, and all the tests are performed using ABAQUS. The geometry of all the models used in ABAQUS are obtained from real experimental tests performed at Volvo Cars, and the material parameters are extracted from the literature.

2 Material and mechanical properties of elastomers

In this chapter follows a brief description of the different types of rubber that are used today as well as the typical mechanical properties that rubber exhibit. A brief history of the rubber will also be presented below.

2.1 Brief history

Today there are thousands of different kinds of rubber used in many different applications, ranging from waterproof shoes to car tires and dishwasher hoses. But these different kinds of rubber typically fall into two different types, namely *natural rubber* and *synthetic rubber* [1]. Generally rubber is also referred to as **elastomers**, which means that they can be stretched out and retain their original geometry when unloaded [7].

Rubber has been known to man for a very long time and was firstly discovered by primitive people in Central and South America in 1600 B.C.E. These people started making bouncing balls for games, and later discovered its waterproofing ability why they started using it to make waterproof clothes. In year 1400 rubber was introduced in Europe, but nobody knew what to do with it. It wasn't until 1764 when people started using the rubber as pencil erasers in England, and in 1824 they started using it as raincoats. Since the material was known to be sticky and smelly at that time the usage was highly limited until a sulfur-based rubber processing called vulcanization was discovered by accident in 1839 by an U.S. inventor called Charles Goodyear. This process made the rubber less sticky, stiffer and more elastic, making it very useful in engineering applications such as vehicle tyres or as shock absorbers [6] [9].

The rubber was entirely made from natural sources until year 1909, which is the year when the first synthetic rubber was created by a team of chemists in Germany lead by Fritz Hofmann. The reason behind the development of synthetic rubber was because it was at this time when the use of bicycles expanded, and the demand of rubber tires increased [2].

2.2 Molecular structure and manufacturing

Below the different manufacturing steps for both natural and synthetic rubber are presented along with the molecular structure of vulcanized rubber.

2.2.1 Natural rubber

Natural rubber is a biosynthetic polymer consisting of very long molecular chains [4] [5]. It is made from a white liquid called **latex**, which is mainly obtained from a tree called *Hevea brasiliensis*, also known as the rubber tree [1] [4]. Raw latex consists of both water and rubber particles [1], and manufacturing natural rubber require different steps which are listed below:

- First step is to obtain the latex from the rubber trees. This is done using a method called **rubber tapping**, which means that a wide V-shaped cut is made into the tree's bark. This results in latex dripping out from the cut, and the rubber liquid

is then collected in cups attached to the tree [1]. The reason behind the V-shaped cut (with an angle of 25-30°) is to "sever the maximum number of latex vessels" (Morton. M 1999, p. 181) [3], which ensures that the maximum amount of latex can be obtained from the tree.

Figure 1. A picture showing a V-shaped cut on a rubber tree, where latex (white fluid) is dripping into a cup. Source: [4]

- In the next step the rubber is filtered and washed, and then the material is reacted with acid in order to make the rubber particles stick together. The rubber is then pressed into slabs and dried, creating unprocessed rubber which mainly consist of the polymer *isoprene* [1]. Since there are minimal bonds between the molecular chains the material shows plastic behaviour when deformed [5].

- In the final steps the unprocessed rubber is turned into a more useful material by making it stiffer and more elastic. Firstly, the unprocessed rubber is pressed using mechanical rollers in order to make it easier to work with (makes it softer and stickier). After that additives and chemicals could be added in order to change the properties of the rubber to meet the desired behaviour [1]. One example is carbon-black filler, which increases the stiffness of the material as well as increasing the resistance to wear [5]. Finally, the rubber is compressed into shape and **vulcanized**, which means that sulfur is added into the rubber mix and then cooked in an industrial pressure cooker to around 140° - 170° C [1] [5]. The sulfur creates chemical links between the molecular chains during vulcanization, creating a highly elastic material [1].

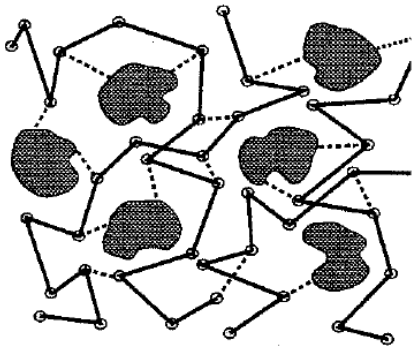

Figure 2. Molecular structure of vulcanized rubber with carbon-black filler. The potato-shaped parts are the carbon-black filler, the solid lines are the polymer chains and the dashed lines represent the crosslinks (sulfur). Source: [5] (Chapter 1.3.1, Page 3)

2.2.2 Synthetic rubber

Synthetic rubber is a man-made rubber with the same molecular structure as natural rubber, and the main raw material used during manufacturing is based on crude oil [7].

There are at least 20 different types of chemicals used today to create synthetic rubber. These chemicals can be combined differently resulting in a lot of different types of synthetic rubbers with different properties and uses [7].

When manufacturing synthetic rubber, petrochemical feedstocks are used as the main ingredient. Different types of gases can also be used when manufacturing synthetic rubber. Two of the most commonly used gases are *butadiene* and *styrene* which creates two different types of synthetic rubbers, namely the **Butadiene Rubber** (BR) and **Styrene Butadiene Rubber** (SBR). Both *butadiene* and *styrene* are by-products from *petroleum*, where *butadiene* is created during petroleum refining and *styrene* is produced during either petroleum refining or in the cooking process. Mixing the different chemicals together with soapsuds in a reactor creates a milky liquid called latex, which is very similar to the latex obtained from the rubber tree. This liquid is then processed in similar way as for the natural rubber, where the liquid is dried, washed and coagulated into unprocessed rubber and finally vulcanized into a stiff and highly elastic material [7].

2.3 Mechanical properties

The most common behaviour know for elastomers are the ability to sustain large deformations and retain its original geometry with minimal permanent deformations. Fillers are sometimes added in the rubber compound to increase stiffness and damping, but the material becomes less elastic in the process. Other properties that are taken advantage of in engineering applications are the vibration damping property and resistance to lubrication [5].

The material behaves non-linear in tension and compression, while it is almost a linear behaviour when in pure shear at relatively low straining [5]. Therefore, the shear

modulus is used instead of Young's modulus when defining elastic material properties for rubber.

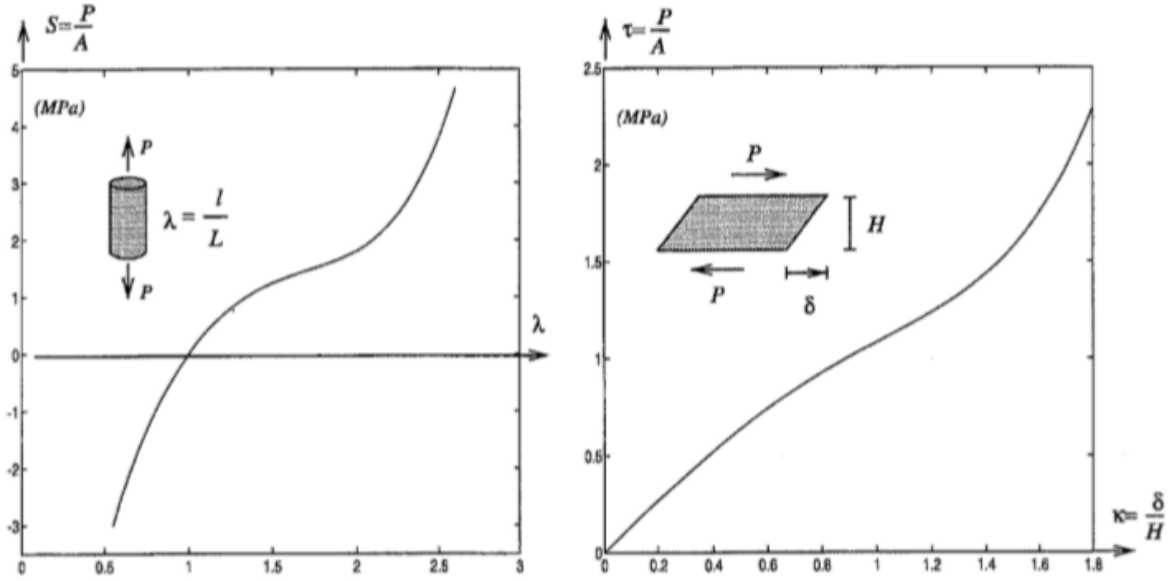

Figure 3. Uniaxial loading (left) and simple shear (right) of a 60 IRHD rubber. Source: [5] (Chapter 1.3.2, Page 7)

When rubber is loaded with a sine or cosine load (dynamic load) there will be a phase shift between the loading and response curves, creating something that is referred to as a *hysteresis loop* [5], see Figure 4.

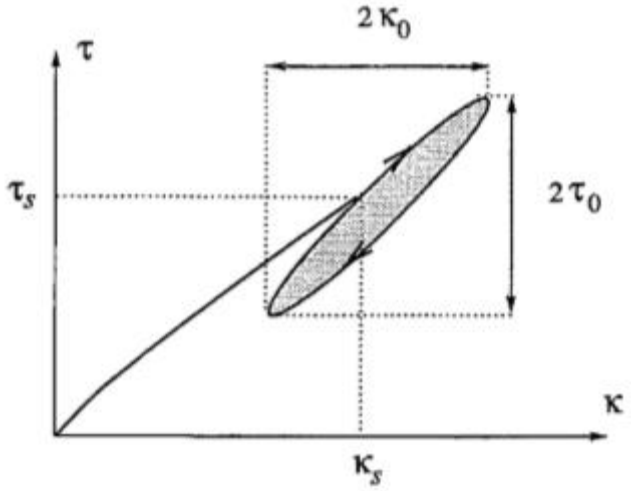

Figure 4. Static and cyclic loading (simple shear) with a typical hysteresis loop. Source: [5] (Chapter 1.3.2, Page 8)

The area enclosed by the loading and unloading curves are referred to as energy-loss in the form of heat. This energy loss causes a decrease of displacement amplitude for an elastomer in free vibration, why damping is introduced as material parameter for rubber. As mentioned before, damping increases when fillers are added in the rubber compound, meaning that the hysteresis loop increases in size [5].

The inclination of the hysteresis loop depends on the frequency of the cyclic loading. This introduces the rate dependent behaviour of rubber, where higher loading frequencies tend to increase the modulus of rubber [8]. The parameter used to describe the inclination of the hysteresis loop is called *dynamic shear modulus* G_{dyn}, and it is always equal or larger than the static shear modulus [5].

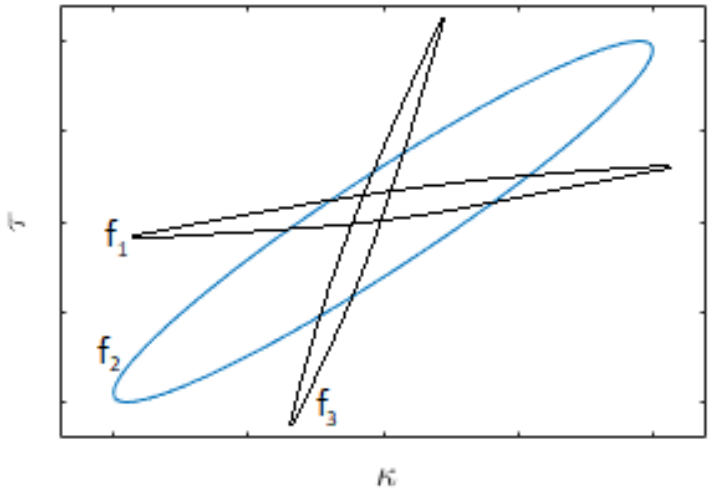

Figure 5. General hysteresis loops for different frequencies (f1 < f2 < f3). The inclinations are heavily exaggerated in this diagram.

The damping is also dependent on the frequency of the cyclic loading. Damping increases with increased frequency, but compared to G_{dyn} damping will start to decrease after a specific frequency [8]. In Figure 6 the general frequency dependence of dynamic shear modulus and damping can be observed.

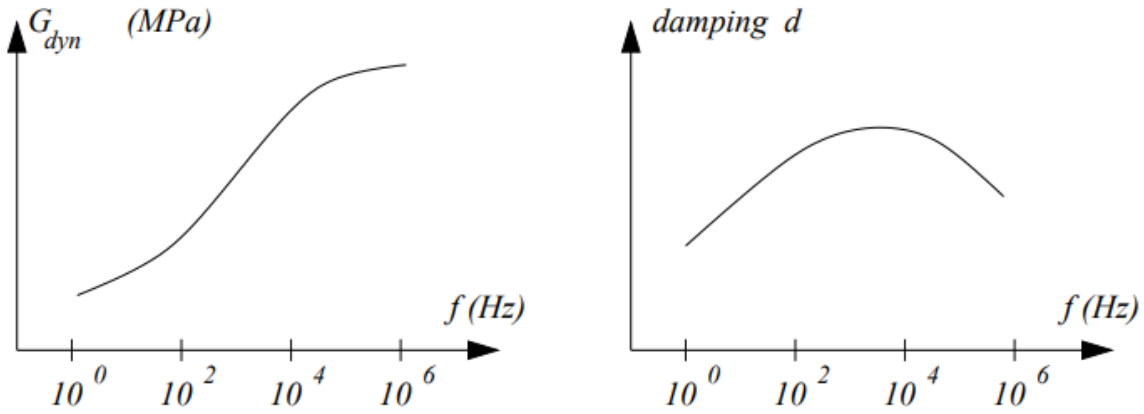

Figure 6. Frequency dependence of shear modulus and damping for a filled rubber.
Source: [8] (chapter 3.5, page 10)

Damping can be interpreted as a relative thickness of the hysteresis loop, and based on the hysteresis loop the damping as well as G_{dyn} is calculated according to following [8]:

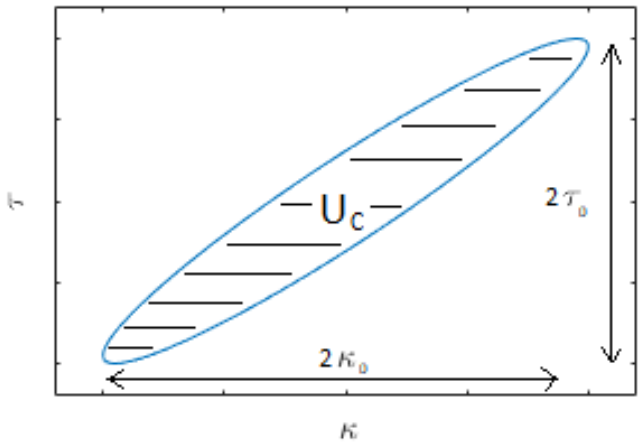

Figure 7. Typical hysteresis loop from a cyclic loading. Similar to Figure 3.2 in [8] (Chapter 3.3, Page 8)

Dynamic shear modulus is defined as

$$G_{dyn} = \frac{\tau_0}{\kappa_0}$$

and damping is defined as

$$d = \sin(\delta) = \frac{U_c}{\pi \kappa_0 \tau_0}$$

with τ_0 being the shear stress amplitude, κ_0 being the shear strain amplitude, U_c being the energy loss per unit volume and δ being the phase angle between loading and response curve.

The dynamic shear modulus and damping also depend on the loading amplitude, which is known as the Fletcher-Gent effect. With an increased amplitude the dynamic shear modulus decreases, while for damping the behaviour is similar as for the frequency dependence [8], see Figure 8.

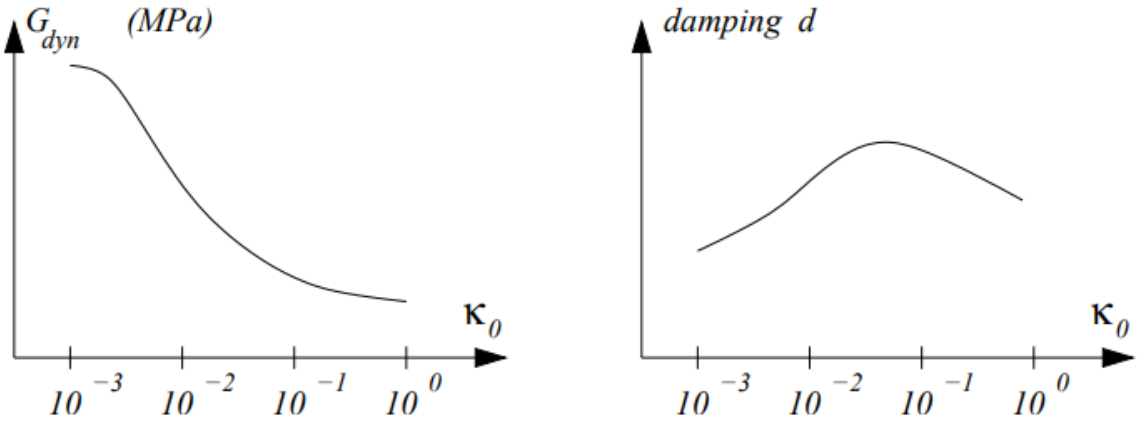

Figure 8. General strain amplitude dependence of shear modulus and damping for filled rubber.
Source: [8] (Chapter 3.6, Page 10)

Mullins effect is also an amplitude dependence which must be considered for elastomers when doing experimental tests, and it is referred to as stress softening. When a previously unloaded specimen is exposed to a cyclic loading up to a specific strain amplitude, the stress level will decrease the first few cycles until it reaches a steady state. And if the same specimen is exposed to a new cyclic loading with a higher strain amplitude the stress will decrease again until it finds a new steady state. From a molecular point of view this can be described as a gradual breakdown of molecular crosslinks as well as changes in rubber network with increasing strain. Compared to the Fletcher-Gent effect it is a more permanent effect of damage [5].

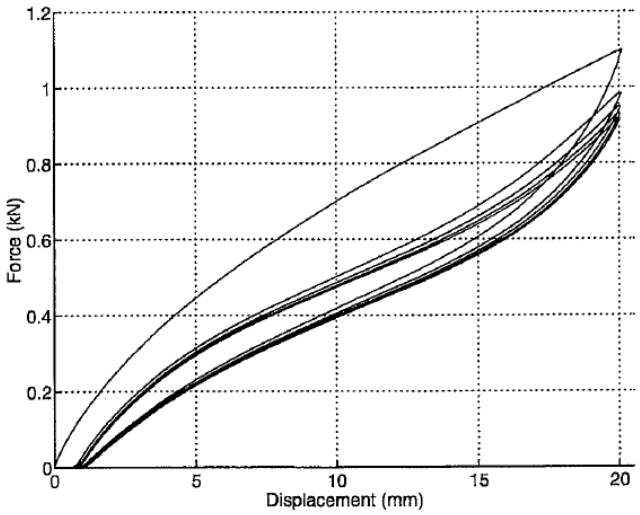

Figure 9. Cyclic loading on a rubber specimen (pure shear) with Mullins effect in action (stress softening).
Source: [5] (Chapter 1.3.2, Page 5)

Another characteristic behaviour for rubber units are the incompressible behaviour, meaning that the volume of the specimen stays the same when it is deformed. A material acquires this type of behaviour when there is a large difference between shear and bulk modulus, i.e. G << B. For rubber material the difference between the shear modulus and bulk modulus are about 1 to 2000, resulting in a nearly incompressible behaviour. A complete incompressible behaviour is therefore often a good assumption when modelling rubber units [5].

3 Non-linear elastic modelling

When modelling non-linear elastic behaviour, the strain energy functions are used as base functions when determining the stiffness of the material as well as the stress levels during deformations. Also, since rubber can sustain very large deformations different types of strain measures can be used when modelling the behaviour of rubber material. The strain measures are presented in Appendix.

3.1 Strain energy functions

A material whose stresses can be defined by a strain energy function is termed as hyperelastic material. Usually when modelling rubber, two different strain energy formats are used, namely the polynomial form and the Ogden form. The difference between the two formats is that the polynomial form contains the elastic constants in a linear dependence while the Ogden form contains the constants in a non-linear dependence as exponents. The Ogden format has shown to be the greater one when fitting the model to experiments, but there is a special choice of the polynomial form with three parameters that gives accurate results when fitting experimental data for natural rubber [5]. In this thesis only the polynomial format will be used in the finite element calculations, why only this format will be presented below.

3.1.1 Strain invariants

The strain measure used in the strain energy functions in this thesis is the left Cauchy-Green deformation tensor **B**, and the theory behind this strain measure can be found in Appendix in this Thesis (final chapter). A general assumption is that the *strain energy per unit volume in the undeformed configuration W* is dependent of all components of the strain measure [5], i.e.

$$W = W(\boldsymbol{B})$$

However, the state of deformation is determined by principal stretches and principal directions, yielding the following [5]

$$W = W(\Lambda_1, \Lambda_2, \Lambda_3, \boldsymbol{n}_1, \boldsymbol{n}_2, \boldsymbol{n}_3)$$

Since rubber is regarded as an isotropic material there will be no directional dependence and *W* is only depended of the principal stretches [5]

$$W = W(\Lambda_1, \Lambda_2, \Lambda_3)$$

The strain energy function should not be dependent on the coordinate system, i.e. the strain energy should always be the same no matter which coordinate system is used. With the principal stretches being dependent on the choice of coordinate system, it is more convenient to use coefficients that are independent of the choice of coordinate system. The strain invariants are therefore introduced [5]:

$$\begin{cases} I_1 = trace(\boldsymbol{B}) = \Lambda_1^2 + \Lambda_2^2 + \Lambda_3^2 \\ I_2 = \frac{1}{2}\left(trace(\boldsymbol{B})^2 - trace(\boldsymbol{B}^2)\right) = \Lambda_1^2\Lambda_2^2 + \Lambda_1^2\Lambda_3^2 + \Lambda_2^2\Lambda_3^2 \\ I_3 = \det(\boldsymbol{B}) = \Lambda_1^2\Lambda_2^2\Lambda_3^2 \end{cases}$$

Where **B** only contains stretches in the principle directions according to below

$$\boldsymbol{B} = \begin{bmatrix} \Lambda_1^2 & 0 & 0 \\ 0 & \Lambda_2^2 & 0 \\ 0 & 0 & \Lambda_3^2 \end{bmatrix}$$

In the case of incompressibility [5] there is no dependence on the third strain invariant since it expresses the volume change, which results in the final form of strain energy which will be used to describe the different strain energy functions used for rubber

$$W = W(I_1, I_2)$$

Because of the condition of incompressibility the values of I_1 and I_2 cannot be chosen freely and are instead restricted. Considering principal directions, the use of the condition $I_3 = 1$ yields the restriction that the first 2 invariants have [5]:

$$\Lambda_3 = \frac{1}{\Lambda_1\Lambda_2}$$

$$\rightarrow \begin{cases} I_1 = \Lambda_1^2 + \Lambda_2^2 + \frac{1}{\Lambda_1^2\Lambda_2^2} \\ I_2 = \Lambda_1^2\Lambda_2^2 + \frac{1}{\Lambda_2^2} + \frac{1}{\Lambda_1^2} \end{cases}$$

Now the values of Λ_1 and Λ_2 can be chosen independently, and Figure 10 shows the restriction that the invariants I_1 and I_2 has for all values of Λ_1 and Λ_2 [5].

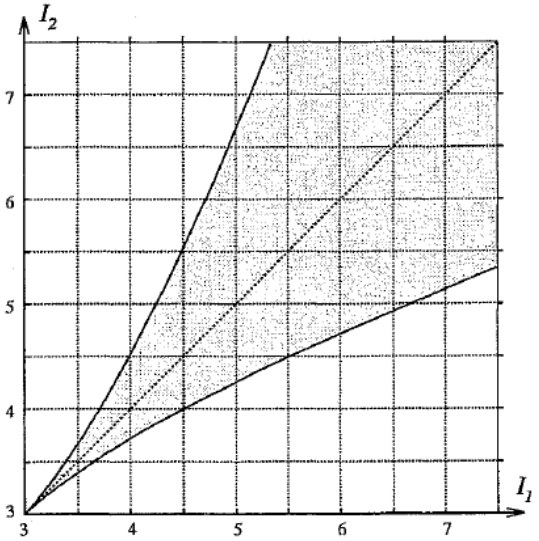

Figure 10. Diagram showing the restricted values (greyed area) of the invariants I_1 and I_2 for incompressible deforamtion.
Source: [5] (Chapter 3.2, Page 25)

3.1.2 Polynomial form

The general form of the polynomial strain energy function [5] is given by the series expansion

$$W = \sum_{i=0,j=0}^{\infty} C_{ij}(I_1 - 3)^i \, (I_2 - 3)^j$$

With C_{ij} being the unknown constants. Note that the sum goes up to infinity in above equation, but usually only a few terms are used. Expanding the expression above with the index sum being less or equal to 3 yields the explicit format [5]

$$W = C_{10}(I_1 - 3) + C_{01}(I_2 - 3) + C_{20}(I_1 - 3)^2 + C_{11}(I_1 - 3)(I_2 - 3) +$$

$$+C_{02}(I_2 - 3)^2 + C_{30}(I_1 - 3)^3 + C_{21}(I_1 - 3)^2(I_2 - 3) +$$

$$+C_{12}(I_1 - 3)(I_2 - 3)^2 + C_{03}(I_2 - 3)^3 + \ldots$$

Taking the first term yields the *Neo-Hooke* material model according to following [5]

$$W = C_{10}(I_1 - 3)$$

With the constant $C_{10} = G/2$ and G is equal to the static shear modulus.

Even though the Neo-Hooke model only contains one term it has shown to give similar results as experiments when it comes to compression and moderate shear [5]. The Neo-Hooke material model is also known as *the first order of deformation*.

Taking the first 2 parameters from the series above yields the *Mooney-Rivlin* material model [5] giving

$$W = C_{10}(I_1 - 3) + C_{01}(I_2 - 3)$$

This material model has shown to be good for natural gum rubber, but less effective for carbon-black-filled rubbers [5].

The second order of deformation is found [5] by taking the first 3 terms in the series above that include the invariants I_1, I_1^2 and I_2 according to below

$$W = C_{10}(I_1 - 3) + C_{01}(I_2 - 3) + C_{20}(I_1 - 3)^2$$

And the *third order of deformation* is found by taking 5 terms in the series that include I_1, I_1^2, I_2, I_1^3 and $(I_1 \cdot I_2)$ giving [5]

$$W = C_{10}(I_1 - 3) + C_{01}(I_2 - 3) + C_{20}(I_1 - 3)^2 + C_{11}(I_1 - 3)(I_2 - 3) + C_{30}(I_1 - 3)^3$$

Yeoh [5] found that the second invariant I_2 in the *third order of deformation* gave bad results for carbon-black-filled natural rubbers. By removing this invariant and only keep the first invariant yields a material model with 3 parameters known as the *Yeoh material model*, and it fits very well with experimental data for carbon-black-filled rubbers giving

$$W = C_{10}(I_1 - 3) + C_{20}(I_1 - 3)^2 + C_{30}(I_1 - 3)^3$$

The parameters in both the Yeoh model and Neo-Hooke model (C_{10}, C_{20} and C_{30}) can be obtained by a shear test or compression and tension test and then use a fitting procedure according to Austrell (1997) [5], which will be explained later in this thesis.

3.2 Constitutive model

The constitutive law for hyperelastic, incompressible and isotropic material can be derived using an energy principle, and the derivation will not be shown here. The constitutive law is given by the following expression [5]

$$\boldsymbol{\sigma} = 2\left(\frac{\partial W}{\partial I_1} + I_1\frac{\partial W}{\partial I_2}\right)\boldsymbol{B} - 2\frac{\partial W}{\partial I_2}\boldsymbol{B}^2 + p\boldsymbol{I} \tag{3.1}$$

Where $\boldsymbol{\sigma}$ is the Cauchy stress tensor, $\boldsymbol{B} = \boldsymbol{F}\boldsymbol{F}^T$ is the left Cauchy-Green deformation tensor, $\boldsymbol{I}$ is a unit matrix and p is the pressure defined as [5]

$$p = \frac{1}{3}(\sigma_{11} + \sigma_{22} + \sigma_{33})$$

By using principle directions in equation (3.1) above it can be shown (by Rivlin [14]) that a relationship between the stress differences can be expressed without using the unknown pressure stress p. The left Cauchy-Green deformation tensor is expressed according to the following [5]

$$\boldsymbol{B} = \boldsymbol{F}\boldsymbol{F}^T = \begin{bmatrix} \Lambda_1^2 & 0 & 0 \\ 0 & \Lambda_2^2 & 0 \\ 0 & 0 & \Lambda_3^2 \end{bmatrix} \qquad \boldsymbol{B}^2 = \begin{bmatrix} \Lambda_1^4 & 0 & 0 \\ 0 & \Lambda_2^4 & 0 \\ 0 & 0 & \Lambda_3^4 \end{bmatrix} \tag{3.2}$$

By inserting the definition of the first invariant (see Ch. 3.1.1) and the definition of the left Cauchy-Greens deformation tensor according to (3.2) into equation (3.1) yields the following relation [5]

$$\begin{cases} \sigma_1 = 2\dfrac{\partial W}{\partial I_1}\Lambda_1^2 + 2\dfrac{\partial W}{\partial I_2}\left((\Lambda_1^2 + \Lambda_2^2 + \Lambda_3^2)\Lambda_1^2 - \Lambda_1^4\right) + p \\ \sigma_2 = 2\dfrac{\partial W}{\partial I_1}\Lambda_2^2 + 2\dfrac{\partial W}{\partial I_2}\left((\Lambda_1^2 + \Lambda_2^2 + \Lambda_3^2)\Lambda_2^2 - \Lambda_2^4\right) + p \\ \sigma_3 = 2\dfrac{\partial W}{\partial I_1}\Lambda_3^2 + 2\dfrac{\partial W}{\partial I_2}\left((\Lambda_1^2 + \Lambda_2^2 + \Lambda_3^2)\Lambda_3^2 - \Lambda_3^4\right) + p \end{cases}$$

Rivlin's relations can now be obtained by subtracting the equations with each other yielding the following with the pressure stress p eliminated [5].

$$\begin{cases} \frac{\sigma_1-\sigma_2}{\Lambda_1^2-\Lambda_2^2} = 2\left(\frac{\partial W}{\partial I_1} + \Lambda_3^2 \frac{\partial W}{\partial I_2}\right) \\ \frac{\sigma_1-\sigma_3}{\Lambda_1^2-\Lambda_3^2} = 2\left(\frac{\partial W}{\partial I_1} + \Lambda_2^2 \frac{\partial W}{\partial I_2}\right) \\ \frac{\sigma_2-\sigma_3}{\Lambda_2^2-\Lambda_3^2} = 2\left(\frac{\partial W}{\partial I_1} + \Lambda_1^2 \frac{\partial W}{\partial I_2}\right) \end{cases} \quad (3.3)$$

Homogenous stress-strain state is usually used when material parameters are characterized, why the constitutive law for homogenous deformations are presented next.

3.2.1 Tension and compression tests

For tension and compression tests the stress – stretch relation can be derived by introducing stress and stretch in the principal directions [5].

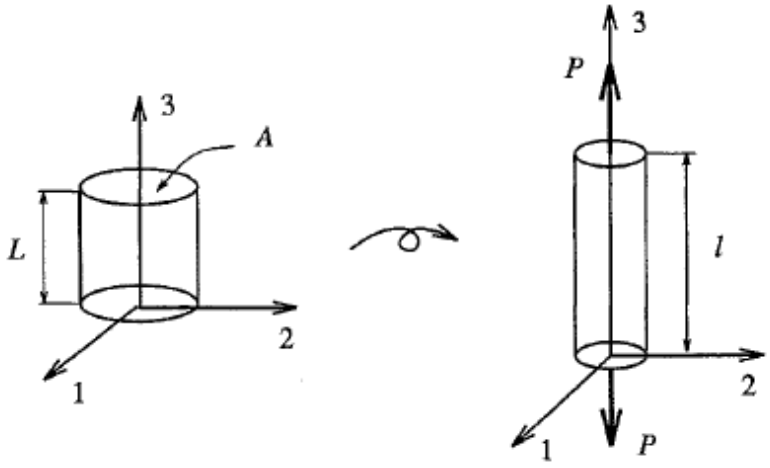

Figure 11. Tension and compression tests.
Source: [5] (Chapter 4.2.1, Page 35)

The stretch in the loading direction is calculated as

$$\Lambda = \frac{L_0 + \delta}{L_0}$$

With L_0 being the initial length of the specimen and δ being the displacement. The stretches in the other directions are determined by the condition of incompressibility which is fulfilled when $\Lambda_1 \cdot \Lambda_2 \cdot \Lambda_3 = 1$, yielding the following [5]

$$\begin{cases} \Lambda_3 = \Lambda \\ \Lambda_1 = \Lambda_2 = \frac{1}{\sqrt{\Lambda}} \end{cases}$$

The invariants for pure tension/compression is determined by inserting the stretch relations above into the general expressions for the strain invariants giving the following [5]

$$\begin{cases} I_1 = \dfrac{2}{\Lambda} + \Lambda^2 \\ I_2 = \dfrac{1}{\Lambda^2} + 2\Lambda \end{cases}$$

Only one stress component is nonzero, and it is calculated according to following [5]

$$\sigma = \frac{P}{a}$$

$$\boldsymbol{\sigma} = \begin{bmatrix} 0 & 0 & 0 \\ 0 & 0 & 0 \\ 0 & 0 & \sigma \end{bmatrix}$$

With a being the deformed cross-sectional area. The relation between the deformed and undeformed area is given by $a = A/\Lambda$ yielding the stress component that is expressed by undeformed cross section as [5]

$$\sigma = \frac{P\Lambda}{A}$$

By using one of the expressions in equation (3.3) the predicted stress-stretch relation can be derived as [5]

$$S = 2\left(\frac{\partial W}{\partial I_1} + \frac{1}{\Lambda}\frac{\partial W}{\partial I_2}\right)\left(\Lambda - \frac{1}{\Lambda^2}\right)$$

With $S = P/A$ being the nominal stress.

3.2.2 Simple Shear

The state of deformation [5] for simple shear is obtained from the deformation gradient, and for simple shear it is given by the following

$$\boldsymbol{F} = \begin{bmatrix} 1 & 0 & \kappa \\ 0 & 1 & 0 \\ 0 & 0 & 1 \end{bmatrix}$$

and the left Cauchy-Green deformation tensor is given by the following

$$\boldsymbol{B} = \boldsymbol{F}\boldsymbol{F}^{\boldsymbol{T}} = \begin{bmatrix} 1+\kappa^2 & 0 & \kappa \\ 0 & 1 & 0 \\ \kappa & 0 & 1 \end{bmatrix} \qquad \boldsymbol{B}^2 = \begin{bmatrix} 1+3\kappa^2+\kappa^4 & 0 & 2\kappa+\kappa^3 \\ 0 & 1 & 0 \\ 2\kappa+\kappa^3 & 0 & 1+\kappa^2 \end{bmatrix}$$

Where $\kappa = tan\theta$ and θ according to Figure 12.

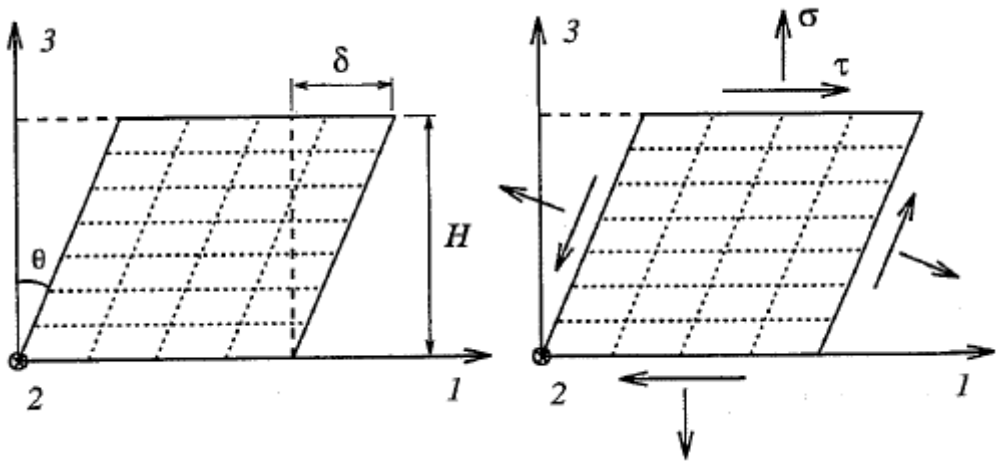

Figure 12. Simple shear.
Source: [5] (Chapter 3.2.2, Page 27)

Using the definition for the strain invariants they are written as [5]

$$\begin{cases} I_1 = tr(\boldsymbol{B}) = 3 + \kappa^2 \\ I_2 = \frac{1}{2}\left(tr^2(\boldsymbol{B}) - tr(\boldsymbol{B}^2)\right) = 3 + \kappa^2 \end{cases}$$

Inserting the Cauchy-Green deformation tensor and invariants into the constitutive law (equation (3.1)) yields the following [5]

$$\begin{bmatrix} \sigma_{11} & \sigma_{12} & \sigma_{13} \\ \sigma_{21} & \sigma_{22} & \sigma_{23} \\ \sigma_{31} & \sigma_{32} & \sigma_{33} \end{bmatrix} = 2\left(\frac{\partial W}{\partial I_1} + (3+\kappa^2)\frac{\partial W}{\partial I_2}\right)\begin{bmatrix} 1+\kappa^2 & 0 & \kappa \\ 0 & 1 & 0 \\ \kappa & 0 & 1 \end{bmatrix} -$$

$$-2\frac{\partial W}{\partial I_2}\begin{bmatrix} 1+3\kappa^2+\kappa^4 & 0 & 2\kappa+\kappa^3 \\ 0 & 1 & 0 \\ 2\kappa+\kappa^3 & 0 & 1+\kappa^2 \end{bmatrix} + p\begin{bmatrix} 1 & 0 & 0 \\ 0 & 1 & 0 \\ 0 & 0 & 1 \end{bmatrix}$$

Compared to linear elasticity the normal stresses are present in all normal directions. However, only two shear stress components are different from zero, namely $\tau = \sigma_{13} = \sigma_{31}$ (see Figure 12). Therefore the shear stress relation for simple shear is found as [5]

$$\tau = 2\left(\frac{\partial W}{\partial I_1} + \frac{\partial W}{\partial I_2}\right)\kappa$$

Simple shear test can be done in two different ways: *quadruple shear* or *double shear* [5].

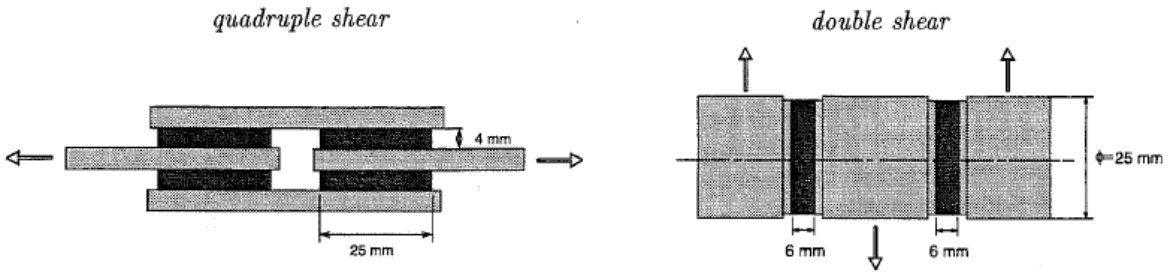

Figure 13. Quadruple shear and double shear specimens. Source: [5] (Chapter 4.3.2, Page 42)

The double shear specimen is made of cylindrical rubber pieces that are attached to cylindrical steel parts. The quadruple shear specimen is made of 4 square rectangular blocks of rubber that are attached to steel (see dimensions in Figure 13). On both tests the force recorded is twice the shear force acting on the rubber pieces. However, the displacement recorded is twice the deformation of a rubber block for the *quadruple shear,* and for *double shear* the displacement recorded is the same as the deformation of a rubber piece [5].

The nominal shear stress is calculated by dividing the shear force *P* with the rubber area *A* that is parallel to the force direction and that is attached to the steel as [5]

$$\tau = \frac{P}{A}$$

Note that for simple shear the rubber area *A* does not change during deformation. The shear strain κ is calculated by dividing the shear displacement δ with the thickness of the rubber *H* as [5]

$$\kappa = \tan\theta = \frac{\delta}{H}$$

yielding the stress-strain relation for simple shear as [5]

$$\frac{P}{A} = 2\left(\frac{\partial W}{\partial I_1} + \frac{\partial W}{\partial I_2}\right)\frac{\delta}{H}$$

4 Modelling general dynamic loads

When modelling the dynamic behaviour of rubber, the rate dependence and amplitude dependence must be considered together with the elastic model. For simple shear it is done by considering two one-dimensional material models. Using a method called the *Overlay method*, these behaviours can be included in two- and three-dimensional finite element models [8]. The finite element method used for the dynamic calculations is presented in Appendix.

4.1 Rate dependence

Rate dependence is modelled using a viscoelastic model. It can be described with a simple one-dimensional model. The simplest model used is the so called *standard linear solid* (SLS) model. The model consists of a Maxwell element coupled in parallel with an elastic spring giving both elastic and viscous properties, and it yields good result for a small range of frequencies. In order to capture a larger range of frequencies multiple Maxwell elements can be connected in parallel resulting in a so-called *generalized Maxwell model* according to Figure 14 [8].

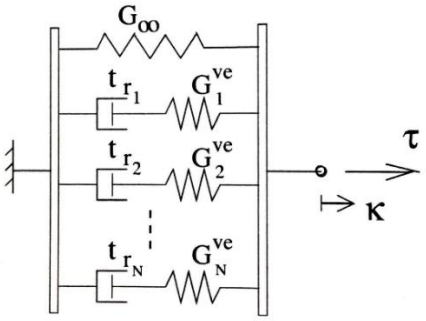

Figure 14. Generalized Maxwell model.
Source: [8] (Chapter 4.2, Page 14)

The total stress from the generalized Maxwell model is calculated by taking the sum of all element stresses in parallel. The stress response is given by the following integral, also known as the hereditary integral [8]

$$\tau_i^{ve}(t) = \int_{-\infty}^{t} G_{R_i}(t-t')\frac{d\kappa}{dt'}dt'$$

Where G_{R_i} is the relaxation modulus for element *i* in the Maxwell model and given by

$$G_{R_i}(t) = G_i^{ve} \cdot e^{-t/t_{r_i}}$$

By the usage of the trapezoidal rule on the hereditary integral the viscoelastic stress for a Maxwell element can be calculated in an incremental form as [8]

$$\Delta\tau_i^{ve} \approx \tau_i^{ve} \cdot \left(e^{-\frac{\Delta t}{t_{r_i}}} - 1\right) + \frac{G_i^{ve}\Delta\kappa}{2} \cdot \left(1 + e^{-\frac{\Delta t}{t_{r_i}}}\right)$$

Where G_i^{ve} and t_{r_i} being material constants for Maxwell elements called *viscoelastic shear modulus* and *relaxation time*, and τ_i^{ve} being the viscoelastic stress from previous step.

4.2 Amplitude dependence

The one-dimensional amplitude dependence of rubber material is modelled using a Coulomb frictional element that is coupled in series with an elastic spring, and the elastoplastic response is based on kinematic hardening. A good fit for a large range of amplitudes can be obtained by using multiple elastoplastic elements in parallel [8], see Figure 15.

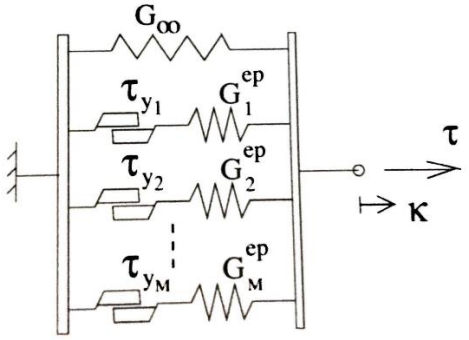

Figure 15. Generalized elastoplastic model.
Source: [8] (Chapter 4.3, Page 15)

This is the simplest elastoplastic model used for elastomers when considering amplitude dependence in dynamic simulations. The stress response for one element can be described in incremental form as [8]

$$\Delta\tau_j^{ep} = \begin{cases} G_j^{ep} \cdot \Delta\kappa & \text{if elastic} \\ 0 & \text{otherwise} \end{cases}$$

The total incremental stress response is then calculated by taking the sum of all parallel elastoplastic elements.

For two- and three-dimensional models the elastoplastic response can either be modelled using kinematic hardening based on the same hyperelastic model as viscoelastic model, or by overlaying multiple non-hardening von Mises models [8].

4.3 Overlay method

From experimental findings [8] it has been shown that amplitude dependence and rate dependence can be considered as two independent behaviours, making it possible to couple the models in parallel and simplifying the calculations greatly. Figure 16 shows an example of a one-dimensional viscoelastic-elastoplastic model [8].

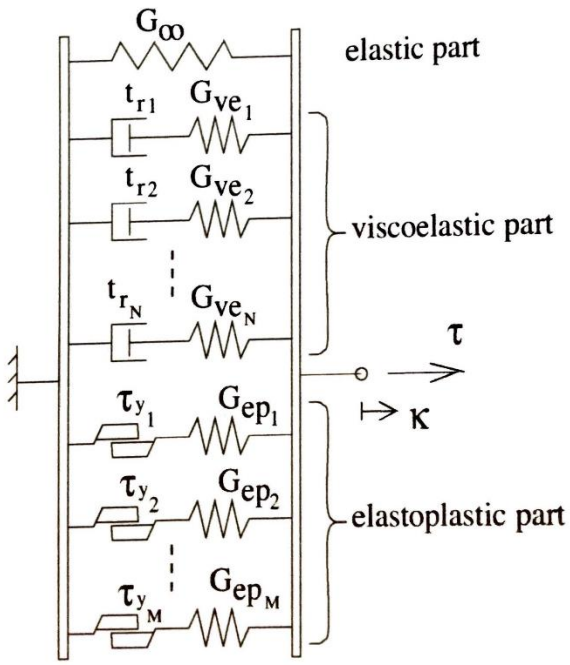

Figure 16. Generalized viscoelastic-elastoplastic model. Source: [8] (Chapter 4.4, Page 16)

The total stress is then obtained by the sum of all stress contributions from all elements [8].

$$\tau = \tau^{e} + \tau^{ve} + \tau^{ep} = \tau^{e} + \sum_{i=1}^{M} \tau_i^{ve} + \sum_{j=1}^{N} \tau_j^{ep}$$

For this to be achieved in finite element analysis the meshes are overlaid in parallel, making it possible to obtain stresses from models that are hard to model in a single mesh. This method is known as the Overlay method and in Figure 17 the principle of the method is shown [8].

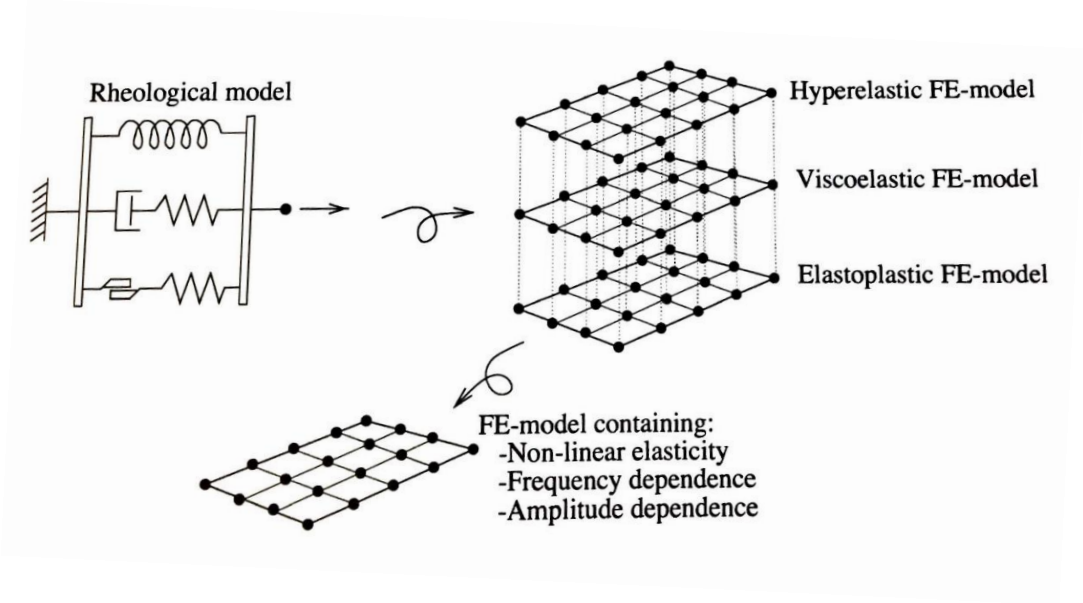

Figure 17. Principle of the overlay method.
Source: [8] (Chapter 4.4, Page 17)

The finite element models are created with the same topology. The stress summation is then achieved by assembling each layer of elements into the same set of nodes [8].

5 Material testing and parameter identification

Different types of experimental testing are performed on rubber in order to classify the hardness of the rubber and determine the static and dynamic material parameters such as hyperelastic constants, dynamic shear modulus and damping. Since rubber manufacturers have many different recipes for rubber mixes the characterization of material parameters requires a lot of laboratory testing. Below different types of experimental testing are introduced as well as the methods used to determine the static and dynamic constants needed for finite element analysis.

5.1 Standard hardness test

The stiffness of vulcanized rubber is classified based on the level of hardness. This is a standard test that is always done for elastomers. There are two different methods used to determine the hardness; the *international rubber hardness degrees* (IRHD), which is also the ISO standard test, and the Shore Hardness test. Both tests give similar results for rubber in the range of 30 – 80 IRHD, which is the range where most of rubber mixes belong. The hardness is determined by measuring the indentation of a needle with a spherical tip or a rigid ball with a constant force applied into a cylindrical rubber piece, where the indentation is then converted into a value of hardness in IRHD scale or Shore Hardness scale [5]. The minimum hardness value is 0 IRHD, which means that the indentation δ goes to infinity, and the maximum hardness value that a specimen can have is IRHD=100, which means that the indentation $\delta = 0$ [5].

The hardness test gives an indirect measure of the elastic modulus. The ISO standard specifies an empirical relation, which is derived by Scott [12], between indentation depth δ in mm, the indenting force F in Newton, the indenter radius r in mm and elastic modulus E in MPa according to following:

$$F = 1.9 \cdot \delta^{1.35} \cdot r^{0.65} \cdot E$$

There is also a relationship between the shear modulus G and hardness value (in IRHD or SHORE) that is constructed by Lindley [13] according to Figure 18, and this is sometimes the only material parameter that is known for a rubber specimen.

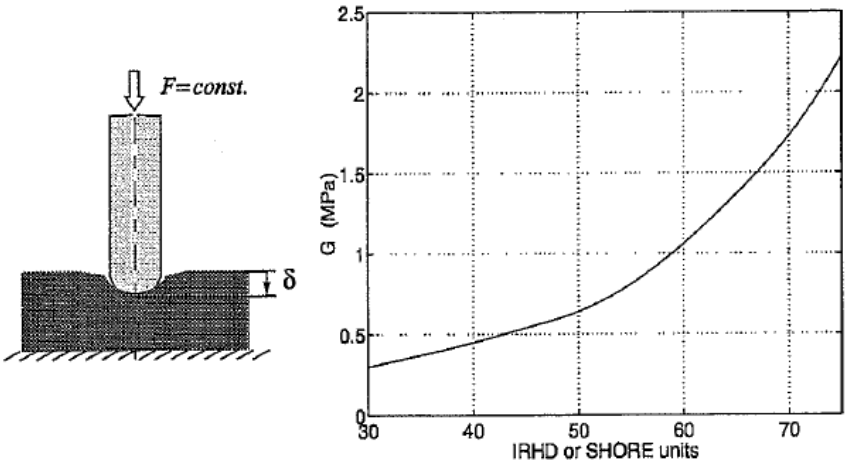

Figure 18. Relationship between shear modulus G and the hardness in IRHD or SHORE units according to Lindley.
Source: [5] (Chapter 1.3.2, Page 6)

5.2 Experimental tests considering homogeneous deformations

In order to obtain the hyperelastic constants and dynamic material parameters, other tests must be done besides the standard hardness test. Traditionally tests that only consider homogenous strain-stress state have been done in order to fit the material models to test data using different fitting procedures.

When it comes to the determination of hyperelastic constants, two different types of experimental tests can be done; lubricated compression-tension test or simple shear test [5].

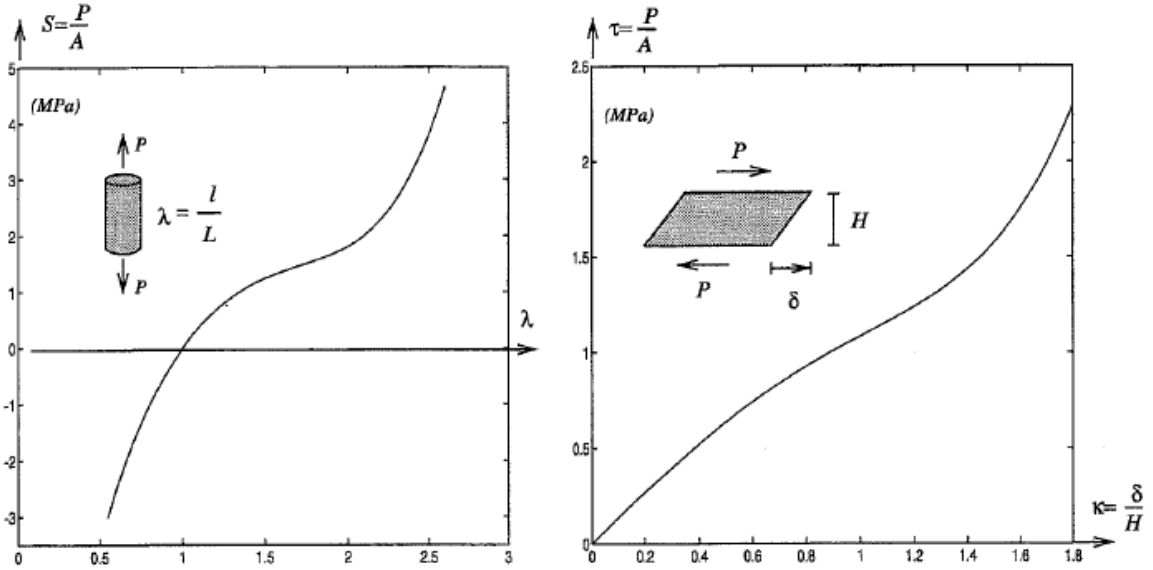

Figure 19. Homogeneous deformations of a 60 IRHD rubber. Left: Uniaxial test. Right: Simple shear.
Source: [5] (Chapter 1.3.2, Page 7)

The material parameters are then determined by a fitting procedure called *least squares*, which is based on fitting the experimental stress-strain relation with the constitutive model used for rubber (example Yeoh model), where the only unknowns are the hyperelastic constants [5].

When it comes to the determination of the dynamic parameters, such as viscoelastic and elastoplastic material parameters, simple shear test is the most commonly used method. The dynamic parameters are then determined using a method called *minimization of relative error*, which is based on finding the minimum of a relative error function ψ containing both experimental data and the unknown material parameters [5].

5.2.1 Hyperelastic constants

The hyperelastic constants are obtained by fitting the hyperelastic model with experimental data using a fitting procedure.

Consider experimental data with *n* numbers of data points obtained from a tension and compression test [5], see Figure 20.

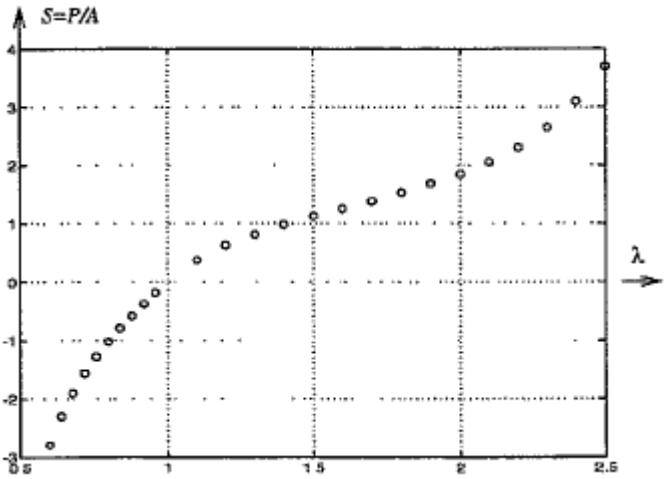

Figure 20. Test data from compression and tension test. Source: [5] (Chapter 5.3.1, Page 59)

Every circle in the diagram correspond to a nominal stress and stretch value (Λ_i, S_i), where $i = 1, \dots, n$. The stress-stretch relation obtained from the constitutive model is then closely fitted to the experimental data points by fulfilling the following condition [5]

$$S_i^{teor} \approx S_i^{exp}$$

Using this condition together with the least squares method a fitting procedure, defined as the minimum of the sum over all datapoints, is introduced [5]

$$\Psi = \sum_{i=1}^{n} \left(S_i^{teor} - S_i^{exp}\right)^2$$

This square of errors can be normalized by rewriting the condition as

$$\frac{S_i^{teor}}{S_i^{exp}} \approx 1$$

Yielding the following sum of squares [5]

$$\Phi = \sum_{i=1}^{n} \left(\frac{S_i^{teor}}{S_i^{exp}} - 1 \right)^2$$

The theoretical stress S_i^{teor} depends on the unknown hyperelastic constants found in the strain energy function $W(I_1, I_2)$. In practice this is usually solved numerically using vectors and matrices. Multiple datapoints are recorded from experimental tests and a linear system of equations are built up according to following [5]

$$\mathbf{Ac} = \mathbf{b}$$

With **A** being a (*n x k*) matrix consisting of the known strain invariants, **c** being a (*k* x 1) vector containing the unknown hyperelastic constants and **b** being a (*n* x 1) vector containing the known forces obtained from experimental tests. *n* is the number of datapoints recorded and *k* is the number of unknown hyperelastic constants. Usually the number of datapoints are much greater than the number of unknown constants, which makes it an overdetermined system of equations. This is easily solved using the method of least squares for matrices and vectors combined with Gauss elimination method [5]

$$\mathbf{A^T A\, c} = \mathbf{A^T b}$$

$$\mathbf{c} = (\mathbf{A^T A}) \setminus (\mathbf{A^T b})$$

5.2.2 Dynamic characterization

The fitting procedure used for the characterization of dynamic parameters can be viewed as a least square minimization of the relative error between experimental data and the one-dimensional viscoelastic-elastoplastic material model [8]. The error function is defined as

$$\psi = (1+\alpha) \sum_{i=1}^{m} \left(\frac{d_{dyn,i} - d_{exp,i}}{d_{exp,i}} \right) + \alpha \sum_{i=1}^{m} \left(\frac{G_{dyn,i} - G_{exp,i}}{G_{exp,i}} \right) \quad (5.1)$$

Where α is a scale factor that makes it possible to decide whether to emphasize a correct modelling of the dynamic shear modulus G_{dyn} or damping d. Either the same scale factor can be chosen for all measurements or individual scale factors can be chosen for each measurement [8].

$G_{dyn,i}$ and $d_{dyn,i}$ are calculated for the material model at different amplitudes and frequencies with m being the number of measurements done. Since $G_{dyn,i}$ and $d_{dyn,i}$ are dependent on the unknown material parameters the relative function becomes a function of the unknown parameters as [8]

$$\psi = \psi\left(G_\infty, G_1^{ve}, t_{r_1}, \dots, G_1^{ep}, \kappa_{y_1}, \dots\right)$$

Since the one-dimensional model consists of three different types of elements (elastic, viscoelastic and elastoplastic element) the total dynamic shear modulus G_{dyn}^{tot} and total damping d_{tot} are calculated as the sum of the contribution from the different elements [8].

Starting with the viscoelastic element, the damping and shear modulus are calculated as [8]

$$d_i = \sin(\delta_i) = \frac{1}{\sqrt{1 + \omega^2 t_{r_i}^2}}$$

$$G_{dyn_1}^{ve} = \frac{G_i^{ve} \omega^2 t_{r_i}^2}{1 + \omega^2 t_{r_i}^2}$$

The different contributions can be plotted in the complex plane according to Figure 21. The static element is also included with the viscoelastic elements [8].

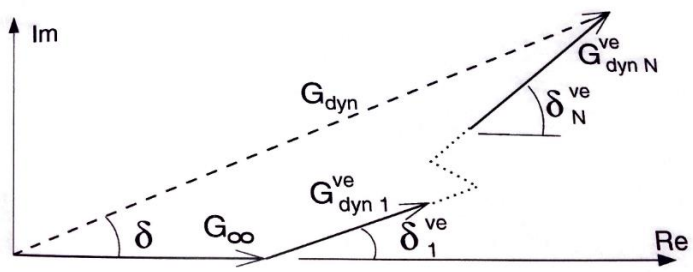

Figure 21. The complex modulus for viscoelastic (Maxwell) elements. The resulting complex modulus is also plotted as a dashed line. Source: [8] (Chapter 3.2, Page 57)

By summing up the total dynamic contribution from the elastic- and all viscoelastic elements results in the following expression [8]

$$G_{dyn}^{ve} = \sqrt{\left(G_\infty + \sum_{i=1}^{N} G_{dyn_i}^{ve} \cos(\delta_i)\right)^2 + \left(\sum_{i=1}^{N} G_{dyn_i}^{ve} \sin(\delta_i)\right)^2}$$

The viscous damping is summed up in similar way as

$$d^{ve} = \frac{1}{G_{dyn}^{ve}} \sum_{i=1}^{N} \frac{G_i^{ve} \omega^2 t_{r_i}^2}{\left(1 + \omega^2 t_{r_i}^2\right)^{3/2}}$$

Moving over to the elastoplastic elements, the dynamic shear modulus is calculated according to following [8]

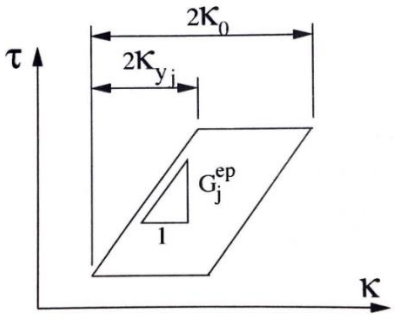

Figure 22. Hysteretic loop for one elastoplastic element.
Source: [8] (Chapter 3.2, Page 58)

$$G_{dyn_j}^{ep} = \begin{cases} \dfrac{G_j^{ep}\kappa_{y_j}}{\kappa_0} & if\ \kappa_0 > \kappa_{y_i} \\ G_j^{ep} & otherwise \end{cases}$$

The total dynamic shear modulus from the elastoplastic elements is then calculated as

$$G_{dyn}^{ep} = \sum_{j=1}^{M} G_{dyn_j}^{ep}$$

And the total plastic damping is calculated according to following

$$d^{ep} = \frac{\sum_{j=1}^{M} U_{c_j}^{ep}}{\pi\kappa_0 \sum_{j=1}^{M} \tau_{0_j}^{ep}}$$

With $U_{c_j}^{ep}$ being the hysteretic work done by one elastoplastic element (the enclosed area by the rhombus in Figure 22) and $\tau_{o_j}^{ep}$ is the stress amplitude for one element and calculated as [8]

$$U_{c_j}^{ep} = \begin{cases} 4\kappa_{s_j} G_j^{ep}\left(\kappa_0 - \kappa_{y_j}\right) & if\ \kappa_0 > \kappa_{y_j} \\ 0 & otherwise \end{cases}$$

$$\tau_{0_j}^{ep} = \begin{cases} G_j^{ep}\kappa_{y_j} & if\ \kappa_0 > \kappa_{y_j} \\ G_j^{ep}\kappa_0 & otherwise \end{cases}$$

Finally, the total contribution from the viscoelastic and elastoplastic elements (note that the viscoelastic part contains the elastic part as well) can be represented in a complex plane according to Figure 23, and using the approximation $\cos(\delta) \approx \cos(\delta^{ep}) \approx \cos(\delta^{ve})$ the total dynamic modulus is calculated according to following [8]

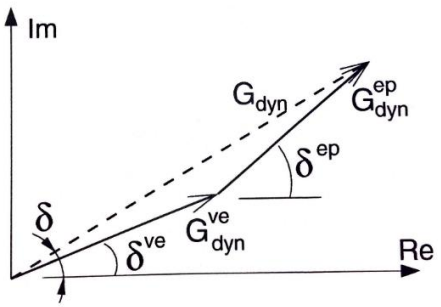

Figure 23. Approximative representation of viscoelastic and elastoplastic response in the complex plane.
Source: [8] (Chapter 3.2, Page 59)

$$G_{dyn} \approx G_{dyn}^{ep} + G_{dyn}^{ve}$$

Using trigonometry, and using $d = \sin(\delta)$ the total damping can be calculated according to following [8]

$$d_{dyn} \approx \frac{G_{dyn}^{ep} d^{ep} + G_{dyn}^{ve} d^{ve}}{G_{dyn}}$$

And by inserting the total damping and dynamic modulus into the error function (5.1) together with experimental data of damping and dynamic shear modulus the material parameters can be obtained. The experimental part in the error function is calculated as

$$G_{\mathrm{exp,i}} = \frac{\tau_{exp,i}}{\kappa_{exp,i}}$$

$$d_{exp,i} = \frac{U_c}{\pi \cdot \kappa_{exp,i} \cdot \tau_{exp,i}}$$

Where $\tau_{exp,i}$ and $\kappa_{exp,i}$ are the nominal shear stresses and strains for different frequencies and amplitudes.

5.3 Modified hardness test

A modification of the standard hardness test has shown to give more information by a small extra effort. The hardness test is modified in a way that instead of applying a constant load and measuring indentation, the force is instead measured for several fixed indentation depths. Previous work done by Austrell [5] has shown that it is possible to obtain the hyperelastic constants by considering energy balance between external work done by the needle and the internal work done by the deformation of the rubber specimen. However, when it comes to the characterization of dynamic parameters it has not been evaluated yet which will be done in this thesis.

5.3.1 Hyperelastic constants

For the static characterization the proposed method is based on an energy balance between external work done by the needle and internal energy which depends on the state of deformation and obtained from a finite element analysis. An assumption is made that the state of deformation is independent of rubber material due to the incompressible behaviour of rubber. This assumption has been proven to be correct in finite element simulations done in previous work [5], see Figure 24.

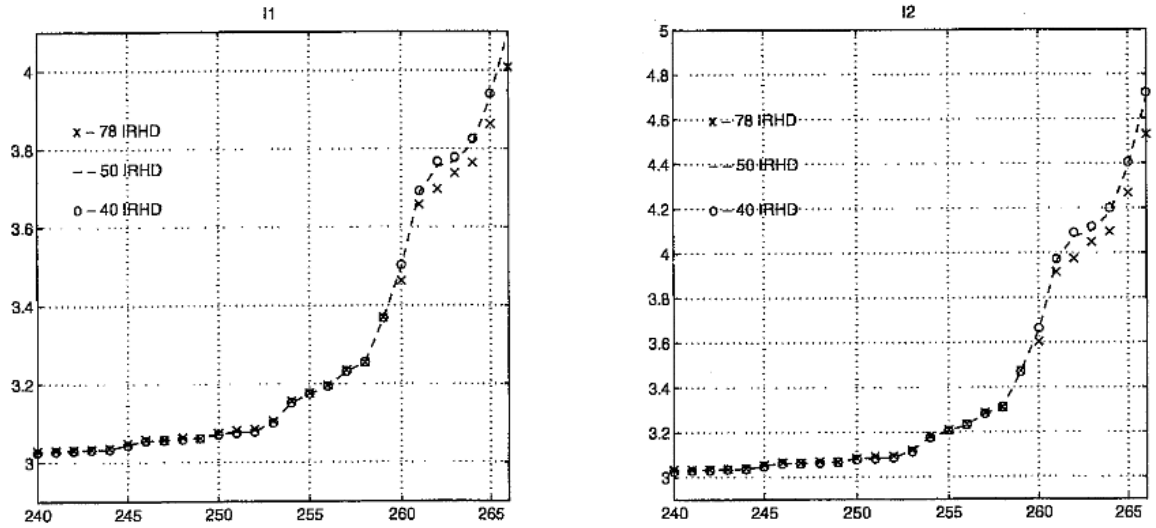

Figure 24. Strain invariants I_1 and I_2 (dimensionless) for the most influenced elements given with element numbers used in the model on the x-axis. Source: [5] (Chapter 7.2.4, Page 95)

This makes it possible to create tabulated values of strain invariants for several indentation depths that can be used to calculate the internal energy without any further computational calculations [5].

The deformed mesh and external force *P* as a function of indentation depth *u* are shown in Figure 25.

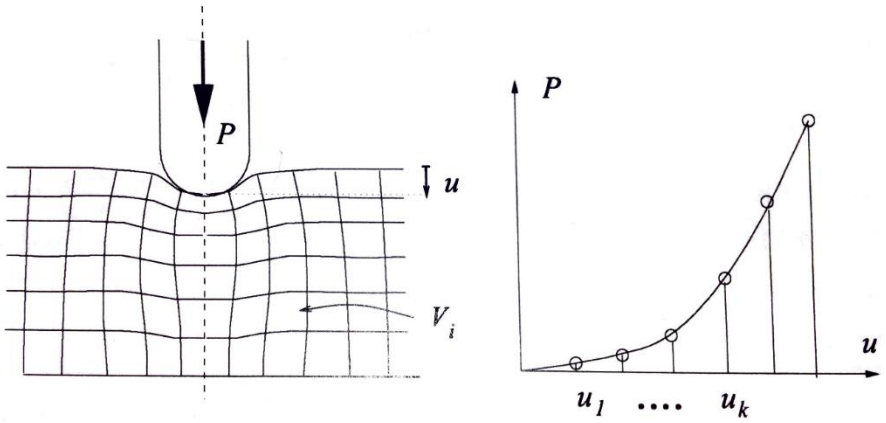

Figure 25. The deformed mesh from and indentation of a needle on the left, and external force P as a function of depth u on the right. Source: [5] (Chapter 7.2.3, Page 92)

The external work done by the indentation force is represented as the area under the curve and calculated by integrating the function *P(u)* from zero to a depth u_k, and the internal work is calculated as the total strain energy stored in the deformed body. From a numerical point of view it is more advantageous to calculate the work done in an incremental form, meaning that the external work and internal energy are calculated as an energy increase when the indentation depth increases from u_k to u_{k+1} [5] resulting in the following equation

$$\int_{u_k}^{u_{k+1}} P(u)du = \sum_{i=1}^{n_e} \left(W_{k+1}^i - W_k^i\right) \cdot V_i$$

Where V_i is the volume of one element and W_k^i is the strain energy density for element *i* at indentation depth u_k. Using a linear approximation for the external work [5] the energy balance can be rewritten as

$$\frac{(P_{k+1}+P_k)}{2} * (u_{k+1} - u_k) = \sum_{i=1}^{n_e} \left(W_{k+1}^i - W_k^i\right) \cdot V_i \quad (5.2)$$

By obtaining values for several different indentation depths a system of equations can be derived with only the hyperelastic constants being unknown, which can be solved using the least square solution for matrices and vectors [5] as

$$\mathbf{A^T A\, c} = \mathbf{A^T b}$$

Where **A** is a matrix or vector (depending on the choice of hyperelastic model) consisting of known values from the strain energy function, **b** being a vector consisting of the incremental external work and **c** being a vector or a scalar consisting of the unknown hyperelastic constant(s) [5].

5.3.2 Dynamic characterization

For the dynamic characterization the proposed method is the same energy balance as for the static characterization. The goal is to obtain an equivalent dynamic shear modulus and damping as for the simple shear test that is later used in the same error function ψ in order to obtain the dynamic material parameters used in finite element analysis. The damping is insensitive to boundary condition why it should be the same as for simple shear [15]. The damping is calculated according to the following

$$d = \frac{U_c}{\pi u_0 P_0}$$

With U_c being the area enclosed by the hysteresis loop and $u_0 = \frac{\Delta u_{k+1}}{2}$ as well as $P_0 = \frac{\Delta P_{k+1}}{2}$.

The dynamic shear modulus can be obtained from the energy balance equation. By using equation (5.2) and adding an extra term $2P_k\Delta u_{k+1}$ on both sides of the equal sign gives the following expression [15]

$$(P_{k+1} + P_k)\Delta u_{k+1} - 2P_k\Delta u_{k+1} = 2\sum_{i=1}^{n_e} \Delta W_{k+1}^i V_i - 2P_k\Delta u_{k+1}$$

With $\Delta u_{k+1} = (u_{k+1} - u_k)$ and $\Delta W_{k+1}^i = \left(W_{k+1}^i - W_k^i\right)$. This gives

$$\Delta P_{k+1}\Delta u_{k+1} = 2\sum_{i=1}^{n_e} \Delta W_{k+1}^i V_i - 2P_k\Delta u_{k+1}$$

The tangential stiffness is introduced, representing the inclination of the force-displacement curve as [15]

$$K^{tang} = \frac{\Delta P_{k+1}}{\Delta u_{k+1}}$$

And inserting this into the modified energy balance equation yields the following

$$K^{tang}(\Delta u_{k+1})^2 + 2P_k\Delta u_{k+1} = 2\sum_{i=1}^{n_e} \Delta W_{k+1}^i V_i \tag{5.3}$$

The simplest way to add the shear modulus in the equation above is by assuming Neo-Hooke model which is directly connected to the shear modulus as $C_{10} = G/2$. Below the strain energy density for neo-Hooke material model is written

$$W = \frac{G}{2}(I_1 - 3)$$

And inserting this into equation (5.3)

$$K^{tang}(\Delta u_{k+1})^2 + 2P_k\Delta u_{k+1} = G\sum_{i=1}^{n_e} \Delta(I_1)_{k+1}^i V_i$$

The assumption is that if K^{tang} is replaced by $K_{dyn}(u, f)$ from experimental data the shear modulus *G* will be replaced by $G_{dyn}(\kappa_{eq}, f)$. The goal is to find $G_{dyn}\left(\kappa_{eq}, f\right)$ as well as the phase angle $\delta(\kappa_{eq}, f)$ with κ_{eq} being the equivalent shear amplitude for the dynamic load and *f* being the load frequency [15].

Alternative method:
There is also a second proposed method for obtaining the equivalent dynamic shear modulus directly from K_{dyn} by multiplying with a scale factor α.

$$\alpha \cdot K_{dyn}(u, f) = G_{dyn}(\kappa_{eq}, f)$$

Hopefully a single value for alpha can be found for all frequencies and amplitudes and that is same for all types of rubber materials. In order to find α several K_{dyn} and G_{dyn} with matching frequencies and amplitudes can be obtained from experimental tests or finite element analysis and two vectors $\boldsymbol{K_{dyn}}$ and $\boldsymbol{G_{dyn}}$ can be built up. And by using

the method of least squares combined with Gauss elimination method, α can be calculated.

$$\alpha \cdot \boldsymbol{K_{dyn}} = \boldsymbol{G_{dyn}}$$
$$\rightarrow \alpha = \left(\boldsymbol{K_{dyn}^T K_{dyn}}\right) \setminus \left(\boldsymbol{K_{dyn}^T G_{dyn}}\right)$$

The problem will be to find a connection between the indentation depth u and shear strain κ. One possibility would be to try a fixed number of amplitudes for modified hardness test, and then loop several different amplitudes for simple shear test and compare the results in order to find the best matching amplitudes. This will however take a long time to do, why it might be easier to assume pure compression for the modified hardness test and put the first invariant for simple shear and pure compression equal;

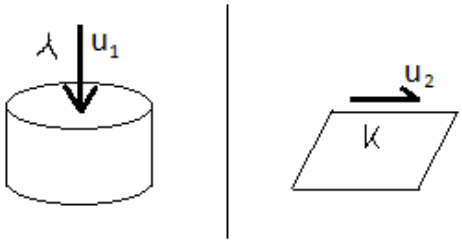

Figure 26. Relationship between compression- and shear amplitude.

$$I_{1,comp} = I_{1,shear}$$
$$I_{1,comp} = \frac{2}{\Lambda} + \Lambda^2 \qquad I_{1,shear} = 3 + \kappa^2$$

By using the nominal strain, the stretch can be rewritten as

$$\Lambda = 1 + \varepsilon \;\rightarrow\; I_{1,comp} = \frac{2}{1+\varepsilon} + (1+\varepsilon)^2$$

And without going too much into detail, the first term in the strain invariant for compression can be simplified into the following

$$\frac{2}{1+\varepsilon} \approx 2 \cdot (1 - \varepsilon + \varepsilon^2)$$

Which simplifies the expression significantly. The connection between the nominal strain and shear strain can now be obtained

$$I_{1,comp} = 2 \cdot (1 - \varepsilon + \varepsilon^2) + (1 + 2\varepsilon + \varepsilon^2) = \ldots\ldots = 3 + 3\varepsilon^2$$

$$3 + \kappa^2 = 3 + 3\varepsilon^2$$

$$\kappa = \sqrt{3} \cdot \varepsilon$$

$$\text{i.e.} \quad \kappa = \sqrt{3} \cdot \frac{u_1}{t_1} \quad \boldsymbol{or} \quad u_2 = \sqrt{3} \cdot u_1 \cdot \frac{t_2}{t_1}$$

With $\kappa = \frac{u_2}{t_2}$ and $\varepsilon = \frac{u_1}{t_1}$. t_1 is the thickness of the compressed rubber and t_2 is the thickness of the sheared rubber.

6 Finite element analysis of modified hardness test

Both static and dynamic parameters were analysed using the finite element software ABAQUS. For the dynamic analysis the overlay method was used in order to include both amplitude dependence and frequency depends on the rubber. The static analysis has already been evaluated in a previous work done by Austrell [5], why only the dynamic analysis has been done in this thesis. The static analysis will however be summarized in this chapter.

Dynamic stiffness and damping were extracted from both simple shear test and modified hardness test and compared. The goal is to be able to find the dynamic shear modulus $G_{dyn}(\kappa_{eq}, f)$ and damping $d(\kappa_{eq}, f)$ computationally from the modified hardness test that is similar to the simple shear test, which can then be used in the error equation presented previously (see equation 5.1, Ch. 5.2.2).

6.1 Static analysis

Previously a method was proposed for the characterization of Yeoh constants from a modified hardness test by using an energy balance equation. This method has already been tested and verified by doing a finite element analysis in [5], and it will be summarized.

6.1.1 Evaluation of hyperelastic parameters

Three different rubber materials with different hardness (IRHD) were used for the analysis: 40 IRHD, 50 IRHD and 78 IRHD. The different rubber materials also had different contents of filler materials added. The hyperelastic constants (Yeoh model) used in the analysis were evaluated in cooperation with different rubber manufacturers from Sweden using homogeneous strain tests in both lubricated compression and simple shear test [5]. The hyperelastic constants are presented in Table 1.

Table 1. Hyperelastic constatns in MPa for 3 different rubber materials. Source: [5] (Chapter 7.2.4, Page 93)

	40 IRHD	50 IRHD	78 IRHD
C_{10}	0.2885	0.5079	1.0543
C_{20}	-0.0394	-0.0593	-0.0779
C_{30}	0.0074	0.0086	0.0241

The rubber disc used for the analysis has a radius of 25 mm and a height of 10 mm. The needle is modelled as a rigid surface with a diameter of 2.5 mm and the contact between the rigid ball and rubber elements is modelled as frictionless corresponding to lubricated indentation test. Because of the symmetry of both the rubber specimen and loading conditions, and because incompressibility is assumed 4-noded axisymmetric elements with hybrid formulations are used for the model (CAX4H) [5]. The model consists of 19 x 14 = 266 elements and is presented in Figure 27.

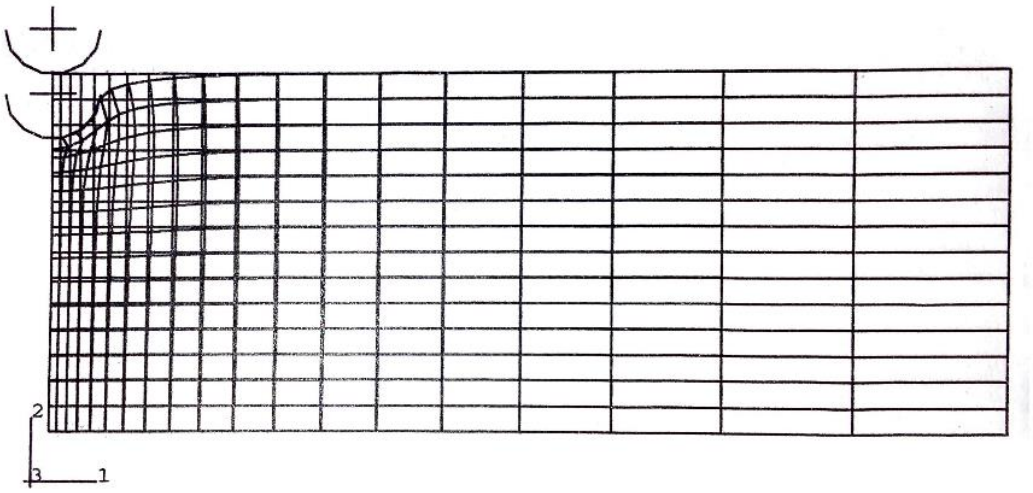

Figure 27. Model with 4-noded axisymmetric elements with hybrid formulation used for static analysis. Radius of rubber disc is 25 mm and diameter of rigid ball is 2.5 mm.
Source: [5] (Chapter 7.2.4, Page 94)

Different indentation depths and reaction forces were then recorded from the rigid surface. The hyperelastic constants are then obtained by using the incremental energy balance [5] according to below

$$\int_{u_k}^{u_{k+1}} P(u)du = \sum_{i=1}^{n_e} \left(W_{k+1}^i - W_k^i\right) \cdot V_i$$

By inserting the Yeoh model in the energy balance the following is obtained

$$\begin{aligned}\int_{u_k}^{u_{k+1}} P(u)du = C_{10} \cdot \Delta_k^{k+1} \sum_{i=1}^{n_e} \left(I_1^i - 3\right) V_i + \\ + C_{20} \cdot \Delta_k^{k+1} \sum_{i=1}^{n_e} \left(I_1^i - 3\right)^2 V_i + \\ + C_{30} \cdot \Delta_k^{k+1} \sum_{i=1}^{n_e} \left(I_1^i - 3\right)^3 V_i\end{aligned}$$

And in matrix formulation it can be rewritten as

$$\mathbf{Ac} = \mathbf{b}$$

With **A** being a (n x 3) matrix consisting of the principal stretches $\left(\Delta_k^{k+1} \sum_{i=1}^{n_e} \left(I_1^i - 3\right)^3 V_i\right)$, **c** being a (3 x 1) vector consisting of the unknown hyperelastic constants and **b** being a (n x 1) vector consisting of the incremental external energy. The row number *n* represents the amount of indentation depths recorded. With the state of deformation being the same for all rubber materials (because of the incompressible behaviour) the

matrix **A** will always be the same for the different test subjects, and it is obtained using the 50 IRHD material parameters [5].

When there are more equations than unknowns, i.e. when $n > 3$, an overdetermined system of equations is obtained. This type of problem is solved using the method of least squares combined with Gauss elimination method [5] according to the following

$$\boldsymbol{A^T A c = A^T b}$$

$$\boldsymbol{c = (A^T A) \setminus (A^T b)}$$

In the finite element analysis, the rigid ball was pressed down to a total displacement of 1.8 mm. The indentation force *P* was recorded at 6 different depths and plotted as a function of the indentation depth according to Figure 28 for the three different rubber materials.

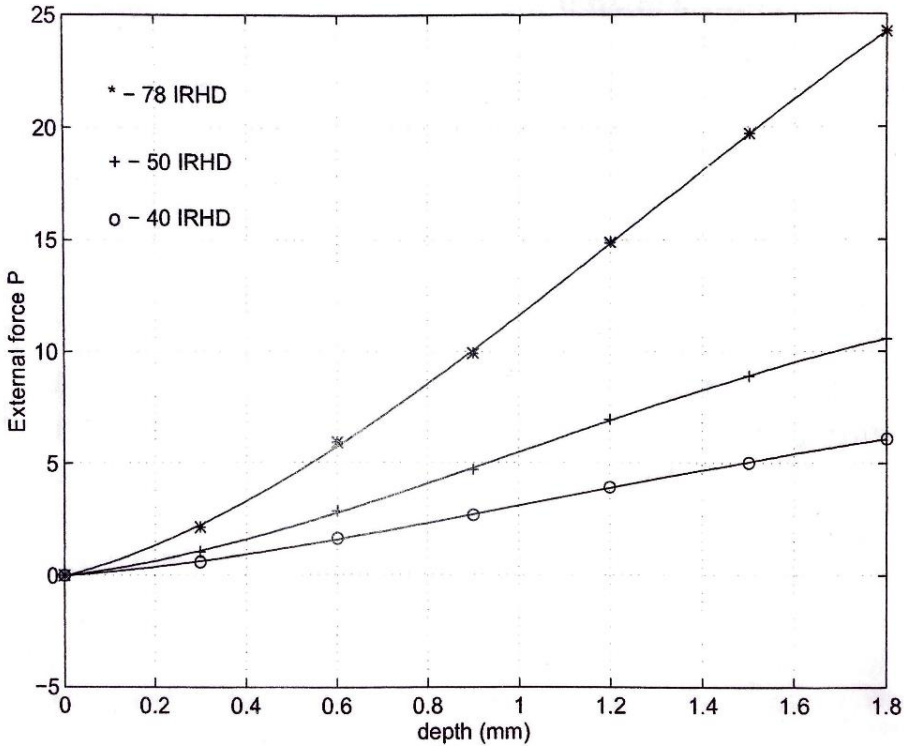

Figure 28. Indentation force P [N] as a function of indentation depth [mm]. Source: [5] (Chapter 7.2.5, Page 96)

The solid lines in Figure 28 are third order polynomials that were fitted to the datapoints. The total external work was then calculated by integrating the third order polynomial from 0 mm indentation to a specific indentation depth [5], and the results are presented in Table 2.

Table 2. Total external work in millijoule [mJ] at different indentation depths. Source: [5] (Chapter 7.2.5, Page 97)

Depth (mm)	40 IRHD	50 IRHD	78 IRHD
0.3	0.082	0.1424	0.2957
0.6	0.4021	0.7020	1.4642

0.9		1.0345	1.8239	3.8174
1.2		2.0204	3.5763	7.5496
1.5		3.3657	5.9570	12.738
1.8		5.0430	8.8918	19.340

With the total external work calculated the incremental external work $\boldsymbol{b}$ can be calculated for the three different rubber materials [5]

$$\boldsymbol{b}_{40} = \begin{bmatrix} 0.0820 \\ 0.3201 \\ 0.6326 \\ 0.9857 \\ 1.3453 \\ 1.6773 \end{bmatrix} \quad \boldsymbol{b}_{50} = \begin{bmatrix} 0.1412 \\ 0.5608 \\ 1.1219 \\ 1.7524 \\ 2.3807 \\ 2.9348 \end{bmatrix} \quad \boldsymbol{b}_{78} = \begin{bmatrix} 0.2957 \\ 1.1685 \\ 2.3532 \\ 3.7622 \\ 5.1579 \\ 6.6026 \end{bmatrix}$$

The strain invariants from the energy balance equation are calculated using finite element analysis at the same indentation depths as in Table 2. As said before, the strain invariants are calculated once using the 50 IRHD material parameters. The incremental strain invariants, or the **A** matrix from the energy balance equation, is set up according to below.

$$\boldsymbol{A} = \begin{bmatrix} 0.2497 & 0.0081 & 0.0005 \\ 1.1158 & 0.1102 & 0.0206 \\ 2.3050 & 0.5596 & 0.2233 \\ 3.6491 & 1.6873 & 1.3063 \\ 5.1895 & 4.9489 & 7.1565 \\ 6.6290 & 11.3516 & 27.6477 \end{bmatrix}$$

Finally, the unknown hyperelastic constant vector $\boldsymbol{c}$ is set up as

$$\boldsymbol{c} = \begin{bmatrix} C_{10} \\ C_{20} \\ C_{30} \end{bmatrix}$$

And by using the method of least squares combined with Gauss elimination method the hyperelastic constants for the different rubber materials are calculated from the energy balance equation and compared with the original constants in Table 1. Below in Table 3 the calculated Yeoh constants are presented [5].

Table 3. Hyperelastic constants in MPa calculated from the matrix format of energy balance equation.
Source: [5] (Chapter 7.2.5, Page 98)

	40 IRHD	**50 IRHD**	**78 IRHD**
$\boldsymbol{C_{10}}$	0.2859	0.5056	1.0616
$\boldsymbol{C_{20}}$	-0.0413	-0.0670	-0.1121
$\boldsymbol{C_{30}}$	0.0091	0.0124	0.0302

By comparing the numbers in both Table 1 and Table 3 it is shown that the calculated constants are very similar to the "correct" hyperelastic constants. A graphical

comparison was also made by looking at the response in compression/tension and simple shear, see Figure 29.

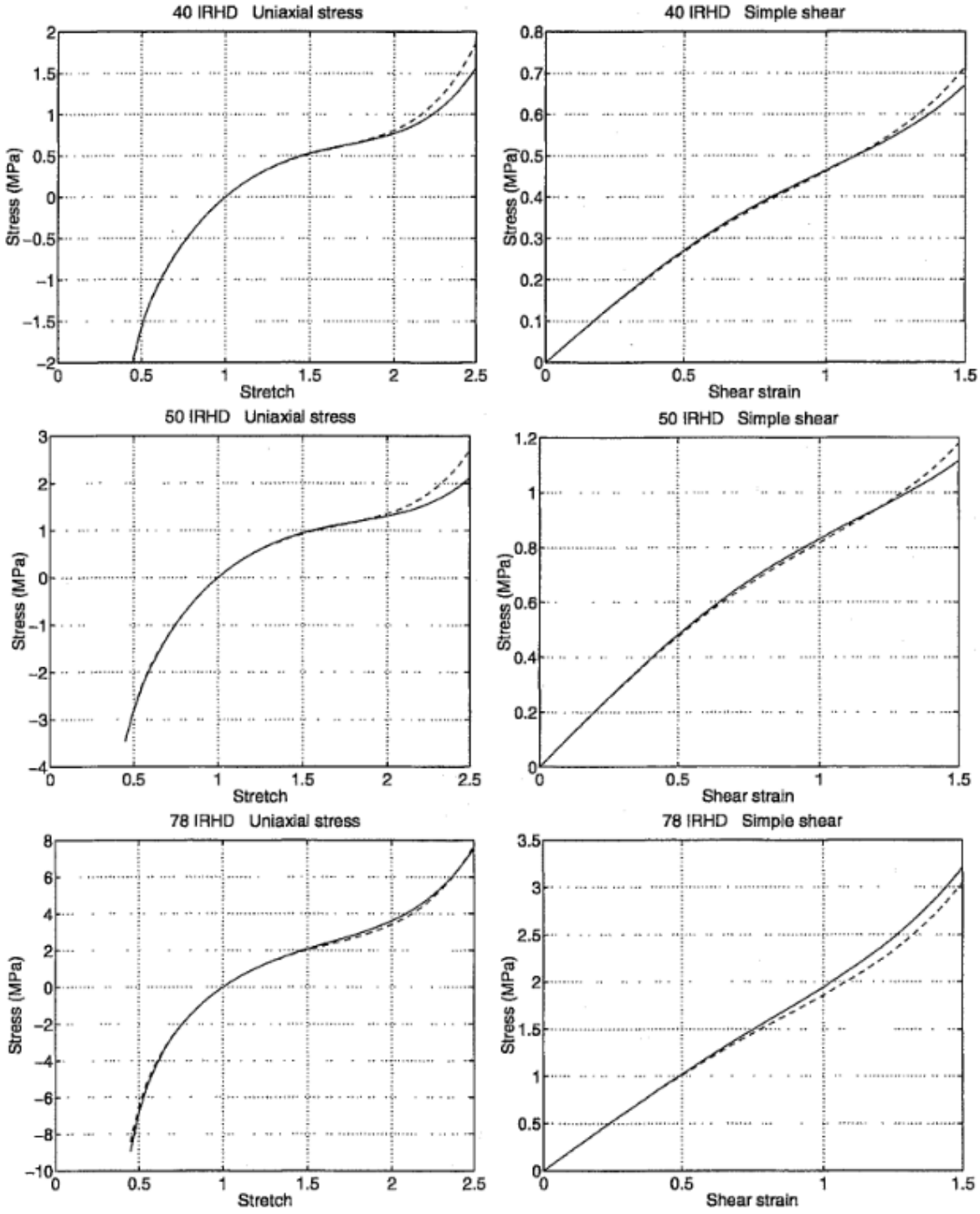

Figure 29. Comparison of hyperelastic constants between modified hardness test (dotted line) and the "correct" hyperelastic constants used in the finite element analysis (solid lines).
Source: [5] (Chapter 7.2.7, Page 100)

From the graphical comparison the calculated hyperelastic constants have very similar behaviour (up to 100% similarity) as the "correct" hyperelastic constants when it comes to stress-strain relation [5].

6.2 Dynamic analysis

6.2.1 Material parameters

Three different synthetic rubber specimens were used in the dynamic analysis: HNBR (hardness ~72), EPDM (hardness ~94) and HGSD85 (hardness ~85). The material parameters were obtained from [8] and are presented in Table 4.

Table 4. Material parameters for three different rubbers. The values are given in [MPa] except for t_r which is given in [s]. Source: [8] (Page 74)

	HNBR	EPDM	HGSD85
G_∞	3.94	9.08	4.52
G_1^{ve}	0.991	1.88	1.21
G_2^{ve}	0.762	1.30	1.38
G_3^{ve}	8.31	3.55	0.190
G_4^{ve}	-	-	6.08
t_{r_1}	0.0105	0.0816	0.0648
t_{r_2}	0.00399	0.00975	0.00622
t_{r_3}	0.000528	0.00130	0.00496
t_{r_4}	-	-	0.000551
G_1^{ep}	7.15	10.1	0.875
G_2^{ep}	3.21	1.49	0.401
G_3^{ep}	0.701	1.89	-
τ_{r_1}	0.0236	0.0477	0.00423
τ_{r_2}	0.0807	0.0303	0.0119
τ_{r_3}	0.0493	0.122	-

Also, since dynamic calculations are performed it is required to add the weight of the rubber in Abaqus, which is assumed to be 1100 kg/m^3 [18].

6.2.2 Material models

The hyperelastic model used is the Yeoh model. In Abaqus the Yeoh model consists of 6 different coefficients according to following [16]

$$W = C_{10}(\overline{I_1} - 3) + c_{20}(\overline{I_1} - 3)^2 + C_{30}(\overline{I_1} - 3)^3 +$$

$$+\frac{1}{D_1}(J^{el} - 1)^2 + \frac{1}{D_2}(J^{el} - 1)^4 + \frac{1}{D_3}(J^{el} - 1)^6$$

D_1, D_2 and D_3 were set to 0 since incompressible behaviour was assumed. The first coefficient governs the initial shear modulus as

$$C_{10} = \frac{G_\infty}{2}$$

The two other coefficients are usually decided using ratios C_{20}/C_{10} and C_{30}/C_{10}, but since these ratios weren't available the following approximative relations were used instead

$$C_{20} = -\frac{G_\infty}{20}$$

$$C_{30} = \frac{3G_\infty}{100}$$

The elastoplastic model used for the rubber is multiple plastic models (meshes) with isotropic hardening. The elastic base used for each plastic model is the Yeoh model. The yield stress for each elastoplastic model is added in Abaqus as von Mises yield stress, and for pure shear it is calculated as

$$\sigma_{v_i} = \tau_{r_i}\sqrt{3}$$

When it comes to viscoelastic model, the parameters included in Abaqus are relaxation time t_r and dimensionless shear relaxation modulus g_R [16] which is calculated as

$$g_{R_i} = \frac{G_i^{ep}}{G_0}$$

Where

$$G_0 = G_\infty + \sum G_i^{ep}$$

6.2.3 Abaqus models for dynamic analysis

Two models have been created in Abaqus; one for simple shear test used as reference, and the other for the modified hardness test.

The simple shear test specimen is modelled as a solid disc. With the deformations being homogenous only a few elements are needed. The model is created using 8-noded 3D-solid elements with 26 elements in total, and on one side the rubber disc is attached to a rigid surface representing the moving steel part from experimental tests. The other side of the rubber specimen is fixed. The dimension of the rubber is the same as for real test specimens used in the labs at Volvo Cars: thickness t = 6 mm and radius R = 12.5 mm.

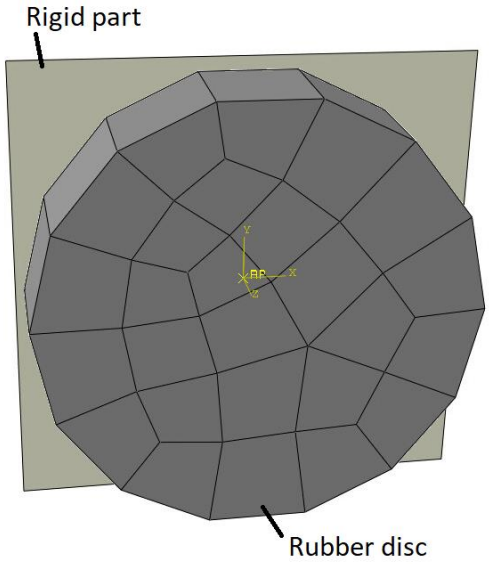

Figure 30. Model used for simple shear test in ABAQUS

The model used for modified hardness test is also modelled as a solid cylinder, but since an energy balance is used for the parameter identification more elements are used. The model is created using 4-noded axisymmetric solid elements with an axisymmetric rigid surface representing the needle pressing down on the rubber. The contact between the rubber and rigid surface is set as frictionless. The rigid surface has a radius of 2.5 mm while the rubber specimen has a radius of 14.25 mm and a thickness of 6 mm, which are the same dimensions as for real test specimens used in the lab at Volvo Cars in Gothenburg. The model can be seen in Figure 31 and has a total of 25x30 = 750 elements.

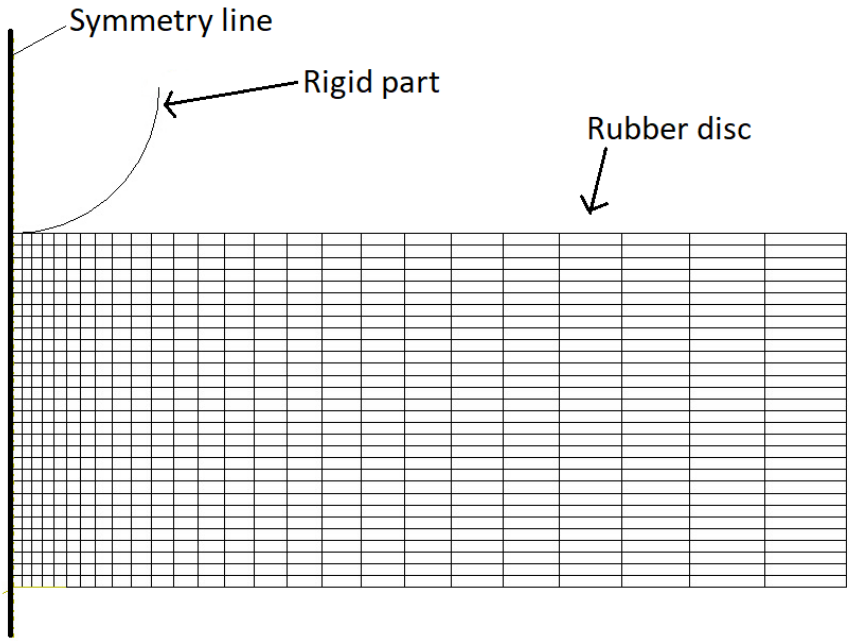

Figure 31. Model used for modified hardness test in ABAQUS.

Since incompressibility is assumed for both models it is required that the elements have a hybrid formulation. With this said the element types used are C3D8H (8-node linear brick with hybrid formulation) for simple shear test specimen and CAX4H (4-node bilinear axisymmetric quadrilateral with hybrid formulation) for modified hardness test specimen [16].

6.2.4 Overlay method

Since ABAQUS can't use viscoelastic and elastoplastic material models for the same mesh the overlay method described earlier must be implemented for both the simple shear test model and the modified hardness test model when evaluating the dynamic parameters.

Four sets of meshes were created using the same nodes for HNBR and EPDM. One mesh was assigned the elastic and viscoelastic material model, and the remaining 3 meshes were used for the elastoplastic material model with isotropic hardening and using Yeoh model as the elastic base.

For HGSD85 three sets of meshes were created instead, with one mesh used for elastic and viscoelastic material model while the remaining meshes were used for the elastoplastic material model.

6.2.5 Evaluation of dynamic shear modulus and damping using the energy balance equation

Both implicit and explicit solvers were tested in ABAQUS when performing the modified hardness test and simple shear test. The responses were identical, but the implicit solver was faster why it was used for the analysis.

Firstly, the needle was prepressed to 1.8 mm (static load), and directly after that the dynamic load was applied in the form of a displacement-controlled sinus load according to the following

$$u = u_0 \cdot \sin(2\pi f)$$

Where u_0 is the amplitude and f is the frequency. The test is performed by combining different frequencies with amplitudes and plotting the frequency and amplitude dependence of damping and dynamic shear modulus in a diagram. The different frequencies used are in a range of 1 – 100 Hz and the different amplitudes used are in a range of 0.06 – 0.72 mm according to Table 5.

Table 5. Frequencies and amplitudes used for the dynamic loads in the finite element analysis.

f (Hz)	u_0 (mm)
1	0.06
5	0.18
20	0.42
50	0.72
100	

In Figure 32 an example of the response curve for the needle can be seen.

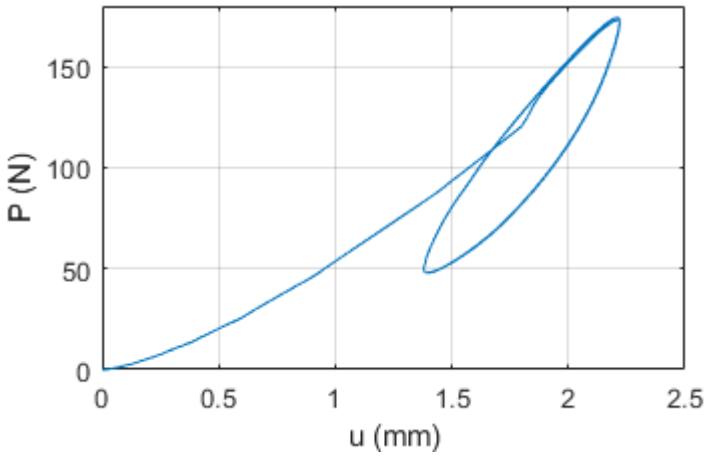

Figure 32. Response curve for a needle pressing into HNBR rubber with a sinus-load (f=20Hz and u_0=0.42mm).

Starting off with the dynamic shear modulus, it is calculated from the energy balance equation by assuming Neo-Hooke material model as

$$K^{dyn}(\Delta u_{k+1})^2 + 2P_k\Delta u_{k+1} = G_{dyn}\sum_{i=1}^{n_e}\Delta(I_1)_{k+1}^{i}V_i$$

$$\rightarrow\ G_{dyn} = \frac{K^{dyn}(\Delta u_{k+1})^2 + 2P_k\Delta u_{k+1}}{\sum_{i=1}^{n_e}\Delta(I_1)_{k+1}^{i}V_i}$$

With $K^{dyn} = \frac{\Delta P_{k+1}}{\Delta u_{k+1}}$ and $\Delta u_{k+1} = u_{k+1} - u_k$

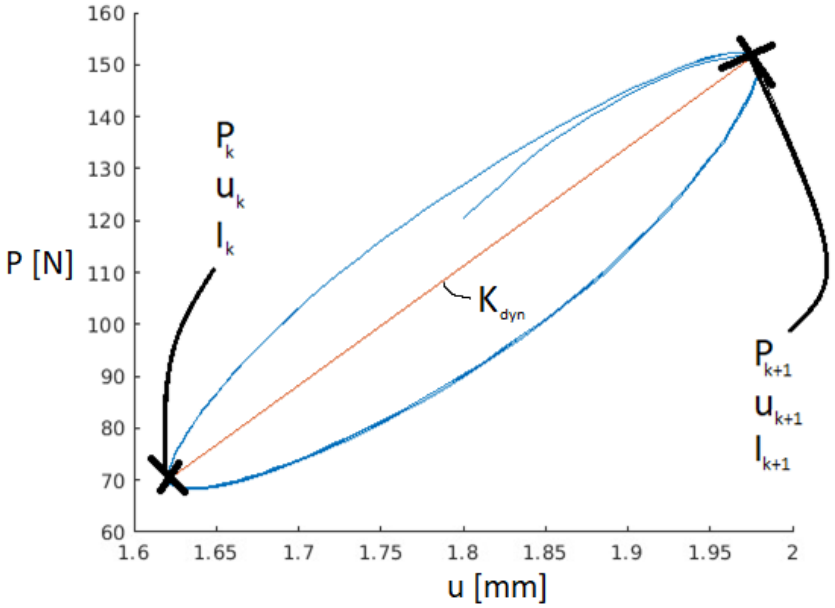

Figure 33. Hysteresis loop (blue curved line) for modified hardness test. Figure showing where to find the different values used in the energy balance equation.

Figure 33 shows the values used in the energy balance equation. According to [15] it is not possible to use the whole model when determining equivalent shear strain, why only the most influenced elements according to Figure 34 are used instead.

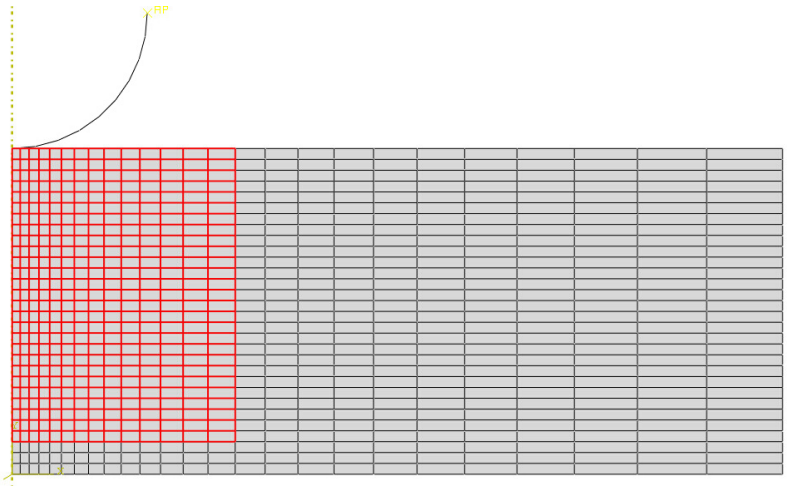

Figure 34. Finite element model used for modified hardness test. The highlighted elements are the most influenced elements when the needle is pressing down into the rubber piece.

Since incompressibility is assumed, the strain invariants are calculated once for the different amplitudes for HNBR and used for all rubber materials. The results are shown in Figure 35.

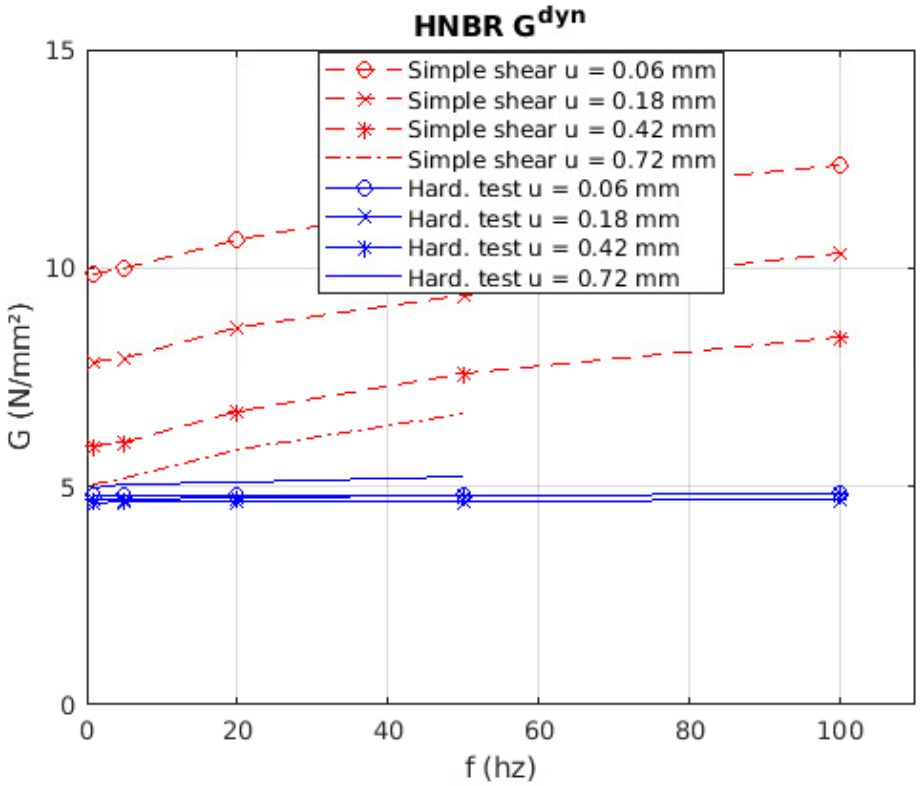

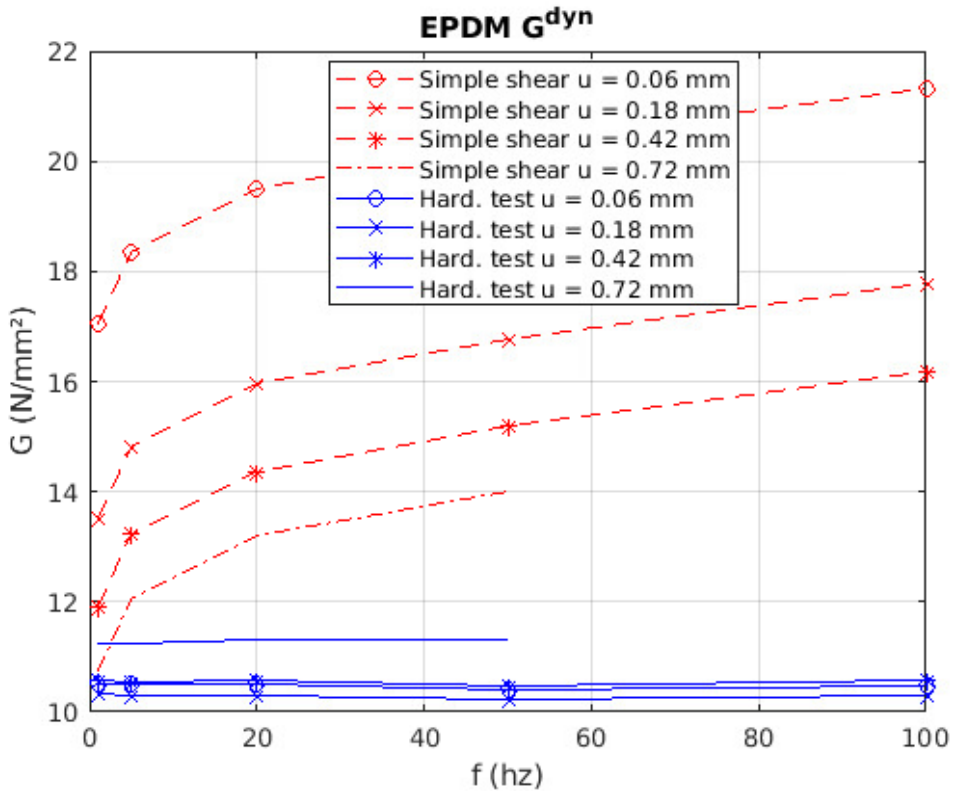

Figure 35. Dynamic shear modulus obtained from energy balance equation (Harndess test) and compared with results from simple shear test.

From the results it is evident that there is neither amplitude nor frequency dependence for the results obtained from the energy balance equation (or a very small dependence). Since the element volume and strain invariants are constant for the different rubber specimens there might be scaling factors that can be used to hit the 'correct' values from the simple shear test and that is the same for all types of rubber materials, but even this gave bad results since the scale factors are varying for the different materials, see Table 6.

Table 6. Ratio between G_{dyn} from the simple shear test and the modified hardness test (energy balance equation).

HNBR Ratio ($G_{simpleShear}$ / $G_{hardTest}$)	1 Hz	5 Hz	20 Hz	50 Hz	100 Hz
u_0 = 0.06 mm	**2.07**	**2.08**	**2.23**	**2.40**	**2.57**
u_0 = 0.18 mm	**1.70**	**1.72**	**1.86**	**2.02**	**2.20**
u_0 = 0.42 mm	**1.26**	**1.28**	**1.42**	**1.59**	**1.75**
u_0 = 0.72 mm	**1.01**	**1.03**	**1.14**	**1.28**	

EPDM Ratio ($G_{simpleShear}$ / $G_{hardTest}$)	1 Hz	5 Hz	20 Hz	50 Hz	100 Hz
u_0 = 0.06 mm	**1.62**	**1.75**	**1.86**	**1.96**	**2.03**
u_0 = 0.18 mm	**1.31**	**1.44**	**1.55**	**1.64**	**1.73**
u_0 = 0.42 mm	**1.13**	**1.25**	**1.36**	**1.45**	**1.53**
u_0 = 0.72 mm	**0.96**	**1.07**	**1.17**	**1.24**	

This was also tested for different amplitudes for the simple shear test ($u = u_0 \cdot \sqrt{3}$) and the results are presented in Table 7.

Table 7. Ratio between G_{dyn} from the simple shear test and the modified hardness test, but with different amplitudes for the simple shear test.

HNBR Ratio ($G_{simpleShear}$ / $G_{hardTest}$)	1 Hz	5 Hz	20 Hz	50 Hz	100 Hz
u_0 = 0.06 mm	**1.86**	**1.88**	**2.07**	**2.23**	**2.41**
u_0 = 0.18 mm	**1.39**	**1.41**	**1.59**	**1.77**	**1.95**
u_0 = 0.42 mm	**1.07**	**1.09**	**1.27**	**1.43**	**1.60**
u_0 = 0.72 mm	**0.90**	**0.91**	**1.07**	**1.20**	

EPDM Ratio ($G_{simpleShear}$ / $G_{hardTest}$)	1 Hz	5 Hz	20 Hz	50 Hz	100 Hz
u_0 = 0.06 mm	**1.44**	**1.56**	**1.67**	**1.77**	**1.85**
u_0 = 0.18 mm	**1.21**	**1.33**	**1.44**	**1.54**	**1.62**
u_0 = 0.42 mm	**1.02**	**1.14**	**1.25**	**1.34**	**1.41**
u_0 = 0.72 mm	**0.89**	**1.01**	**1.10**	**1.17**	

6.2.6 Alternative method

With the energy balance equation not working very well for the dynamic characterization the alternative method is analyzed instead. The tangential stiffness K_{dyn} is directly compared to the dynamic shear modulus obtained from the simple shear test by assuming a linear connection between the two quantities. By calculating multiple K_{dyn} and G_{dyn} two vectors can be built up, and the ratio that connects the two quantities is then calculated using the method of least squares combined with Gauss elimination method;

$$\alpha \cdot \boldsymbol{K_{dyn}} = \boldsymbol{G_{dyn}}$$

$$\rightarrow \alpha = \left(\boldsymbol{K_{dyn}^T K_{dyn}}\right) \setminus \left(\boldsymbol{K_{dyn}^T G_{dyn}}\right)$$

Firstly, the same amplitudes are used for both simple shear test and modified hardness test, and the results are presented in Figure 36.

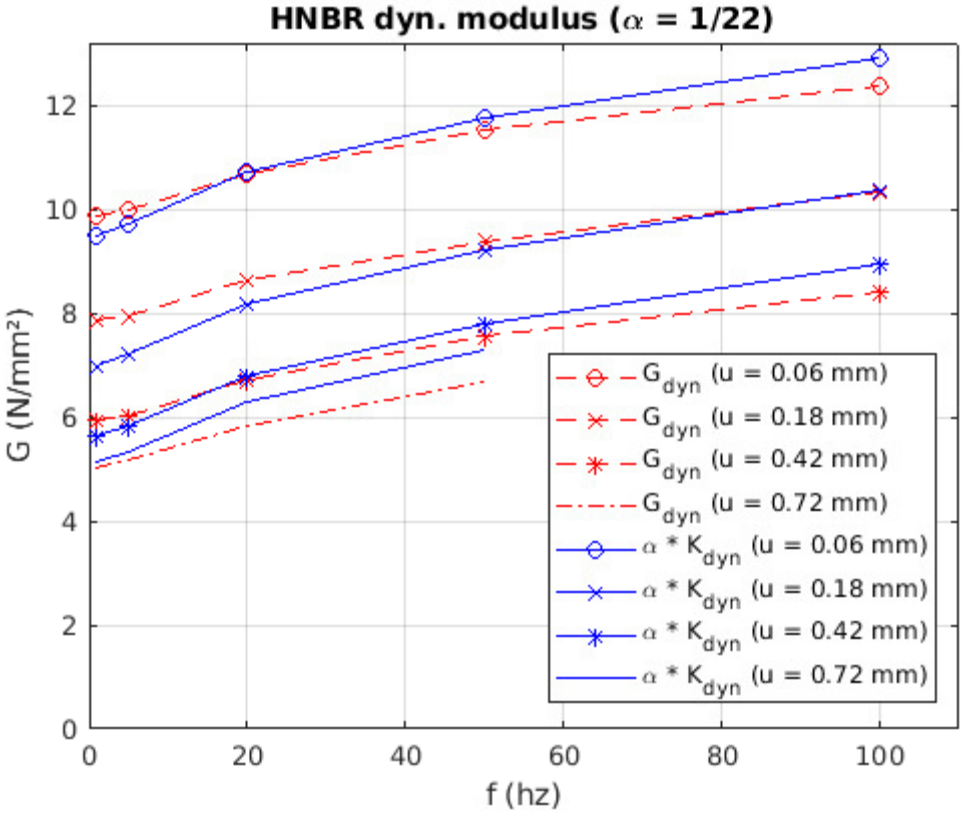
HNBR dyn. modulus (α = 1/22)
G (N/mm²)
f (hz)
0
2
4
6
8
10
12
0
20
40
60
80
100
G_dyn (u = 0.06 mm)
G_dyn (u = 0.18 mm)
G_dyn (u = 0.42 mm)
G_dyn (u = 0.72 mm)
α * K_dyn (u = 0.06 mm)
α * K_dyn (u = 0.18 mm)
α * K_dyn (u = 0.42 mm)
α * K_dyn (u = 0.72 mm)

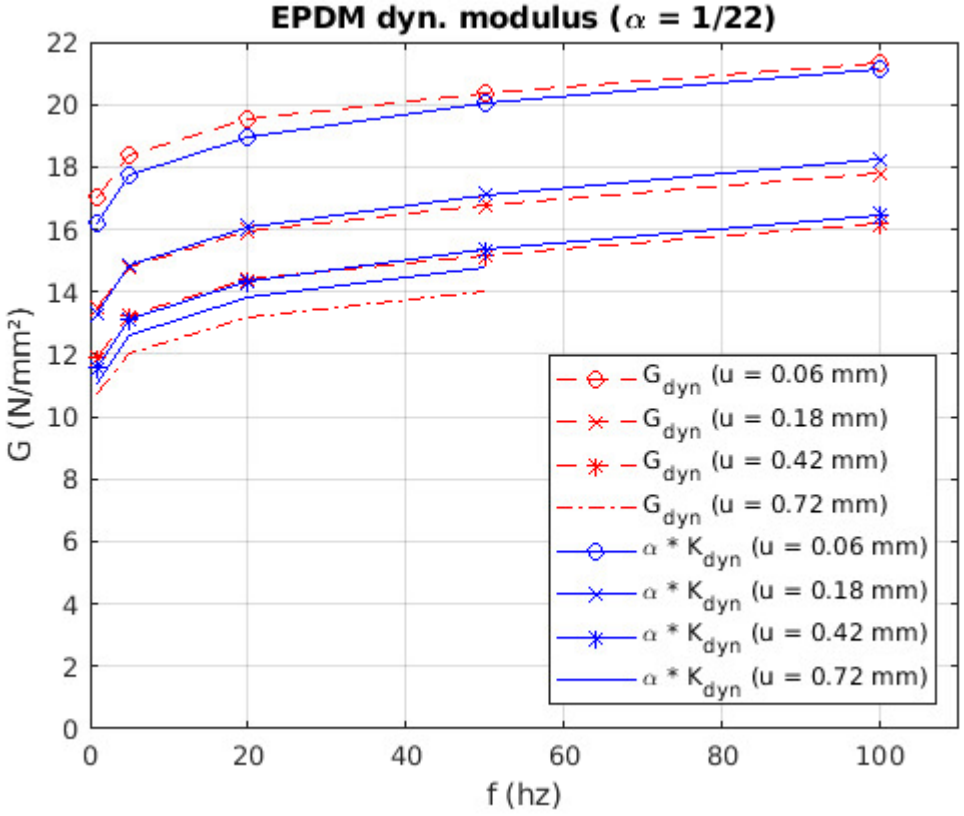
EPDM dyn. modulus (α = 1/22)
G (N/mm²)
f (hz)
0
2
4
6
8
10
12
14
16
18
20
22
0
20
40
60
80
100
G_dyn (u = 0.06 mm)
G_dyn (u = 0.18 mm)
G_dyn (u = 0.42 mm)
G_dyn (u = 0.72 mm)
α * K_dyn (u = 0.06 mm)
α * K_dyn (u = 0.18 mm)
α * K_dyn (u = 0.42 mm)
α * K_dyn (u = 0.72 mm)

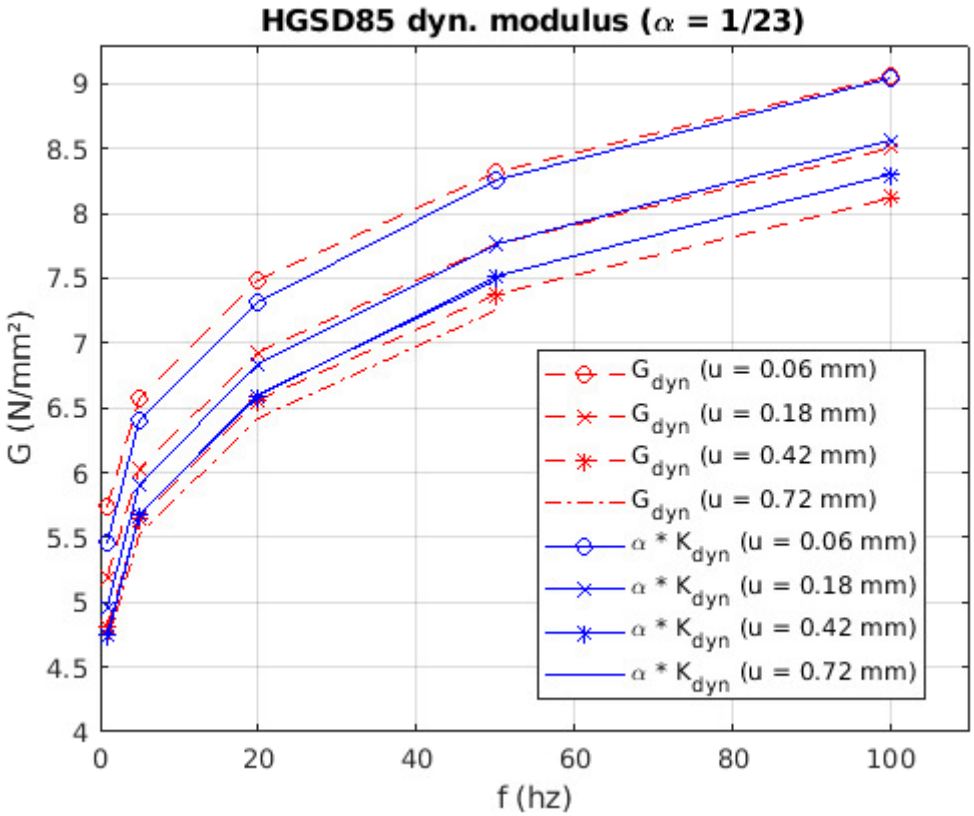

Figure 36. Dynamic modulus for modified hardness test (blue solid lines) and simple shear test (red dashed lines), alternative method with same set of amplitudes.

From the results in Figure 36 it is evident that there is an obvious relationship between the tangential stiffness K_{dyn} and dynamic shear modulus G_{dyn}, and the scaling factor α is tending to hit (almost) the same constant for the different rubber materials. However, the lines don't seem to align perfectly which is probably due to the amplitudes not matching. Previously a relationship between the amplitudes was obtained by assuming pure compression for modified hardness test according to following

$$I_1^{comp} = I_1^{shear}$$

$$\rightarrow \kappa = \frac{u_{comp}}{t} \cdot \sqrt{3}$$

or

$$u_{shear} = u_{comp} \cdot \sqrt{3} \quad (same\ thickness)$$

A finite element analysis was therefore made with the assumed relationship between the amplitudes according to above and the following results were obtained.

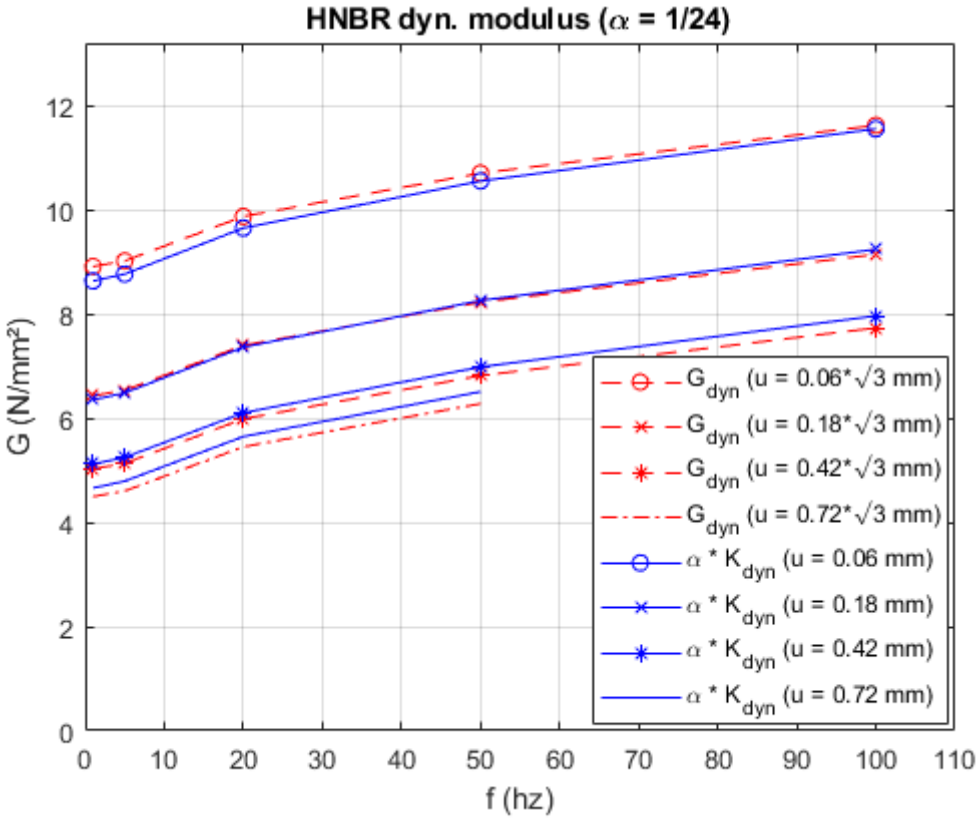
HNBR dyn. modulus (α = 1/24)
G (N/mm²)
f (hz)
G_dyn (u = 0.06*√3 mm)
G_dyn (u = 0.18*√3 mm)
G_dyn (u = 0.42*√3 mm)
G_dyn (u = 0.72*√3 mm)
α * K_dyn (u = 0.06 mm)
α * K_dyn (u = 0.18 mm)
α * K_dyn (u = 0.42 mm)
α * K_dyn (u = 0.72 mm)

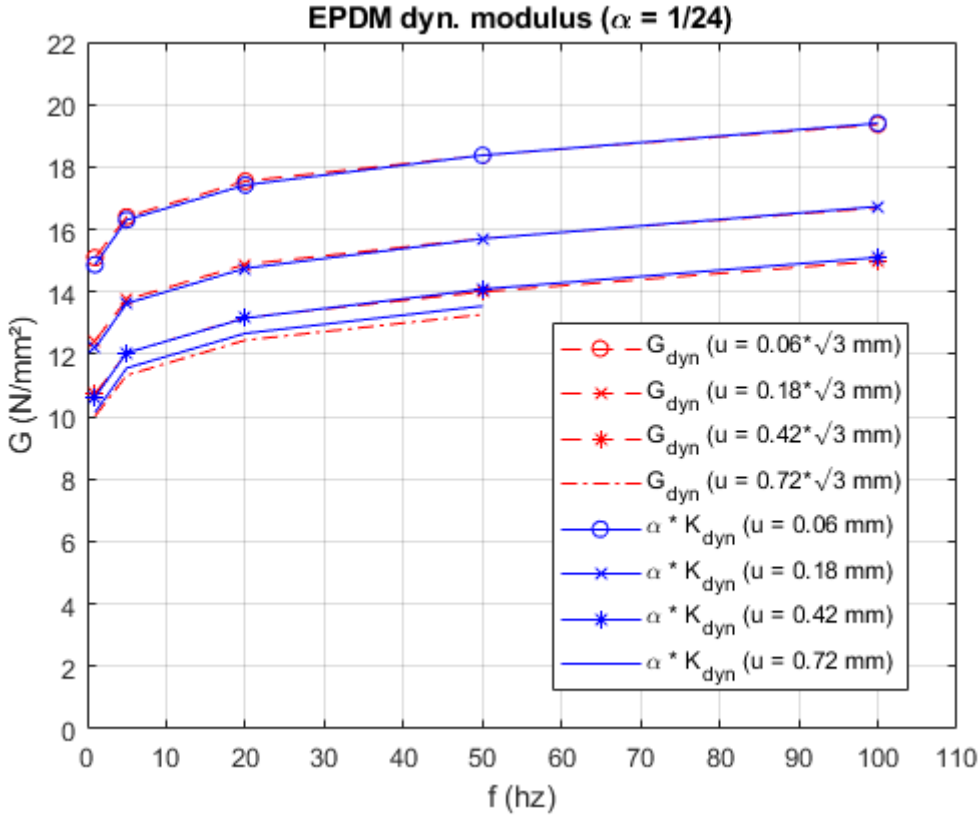
EPDM dyn. modulus (α = 1/24)
G (N/mm²)
f (hz)
G_dyn (u = 0.06*√3 mm)
G_dyn (u = 0.18*√3 mm)
G_dyn (u = 0.42*√3 mm)
G_dyn (u = 0.72*√3 mm)
α * K_dyn (u = 0.06 mm)
α * K_dyn (u = 0.18 mm)
α * K_dyn (u = 0.42 mm)
α * K_dyn (u = 0.72 mm)

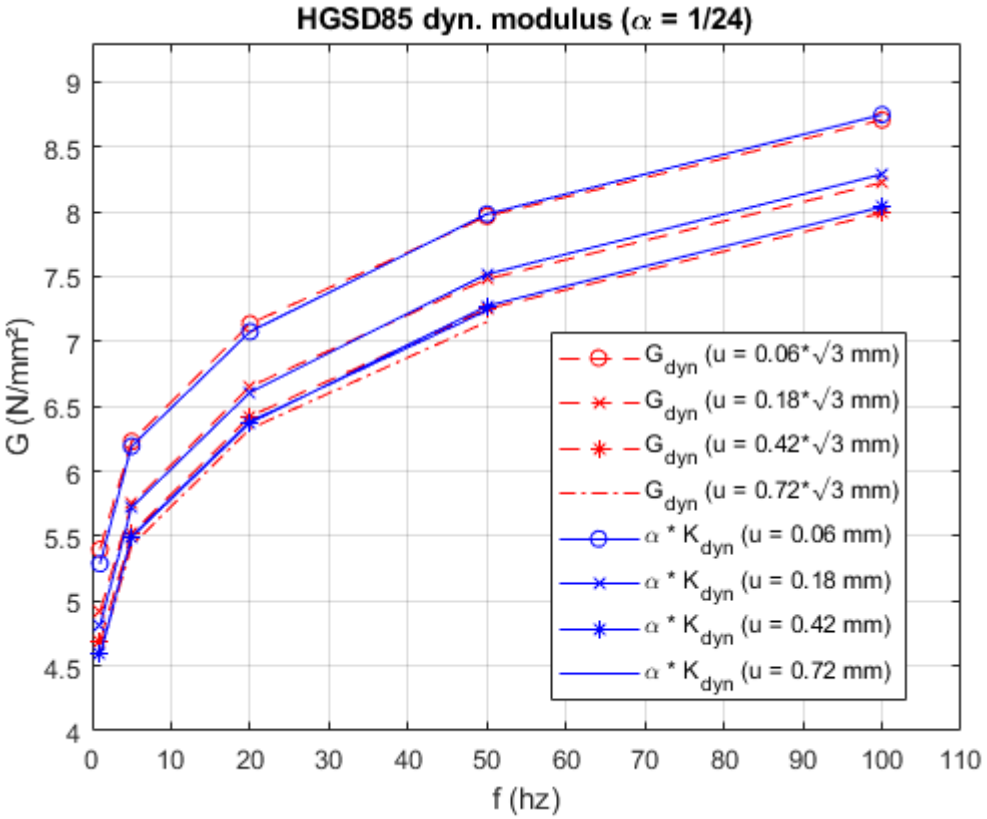

Figure 37. Dynamic modulus for modified hardness test (blue solid lines) and simple shear test (red dashed lines), alternative method with different sets of amplitudes.

From the results in Figure 37 it is now possible to see that the solid blue lines and dashed red lines from the different tests fit each other better than before. The constant α is also the same for all the tested rubber materials.

Next up is damping, and it is calculated for simple shear test as

$$d = \frac{U_c}{\pi \kappa_0 \tau_0}$$

And for modified hardness test as

$$d = \frac{U_c}{\pi u_0 P_0}$$

Firstly, the damping is obtained for identical amplitudes for simple shear test and modified hardness test. The results from the finite element analysis are presented in Figure 38.

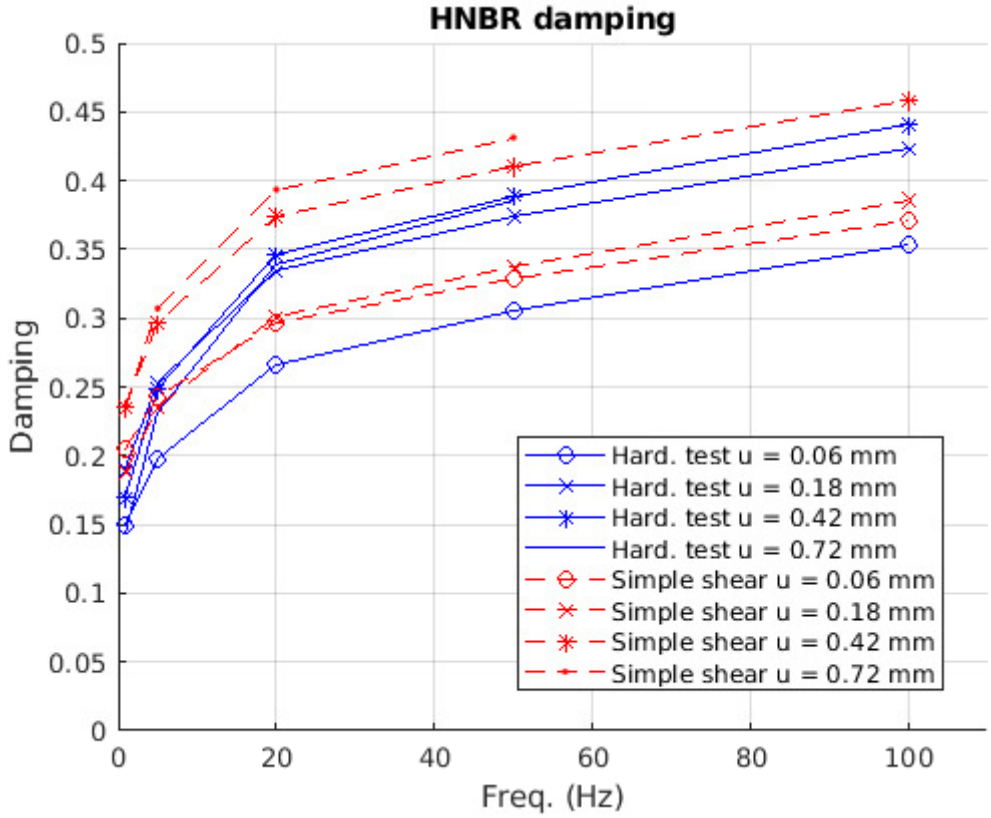
HNBR damping
Damping
Freq. (Hz)
0
0.05
0.1
0.15
0.2
0.25
0.3
0.35
0.4
0.45
0.5
0
20
40
60
80
100
Hard. test u = 0.06 mm
Hard. test u = 0.18 mm
Hard. test u = 0.42 mm
Hard. test u = 0.72 mm
Simple shear u = 0.06 mm
Simple shear u = 0.18 mm
Simple shear u = 0.42 mm
Simple shear u = 0.72 mm

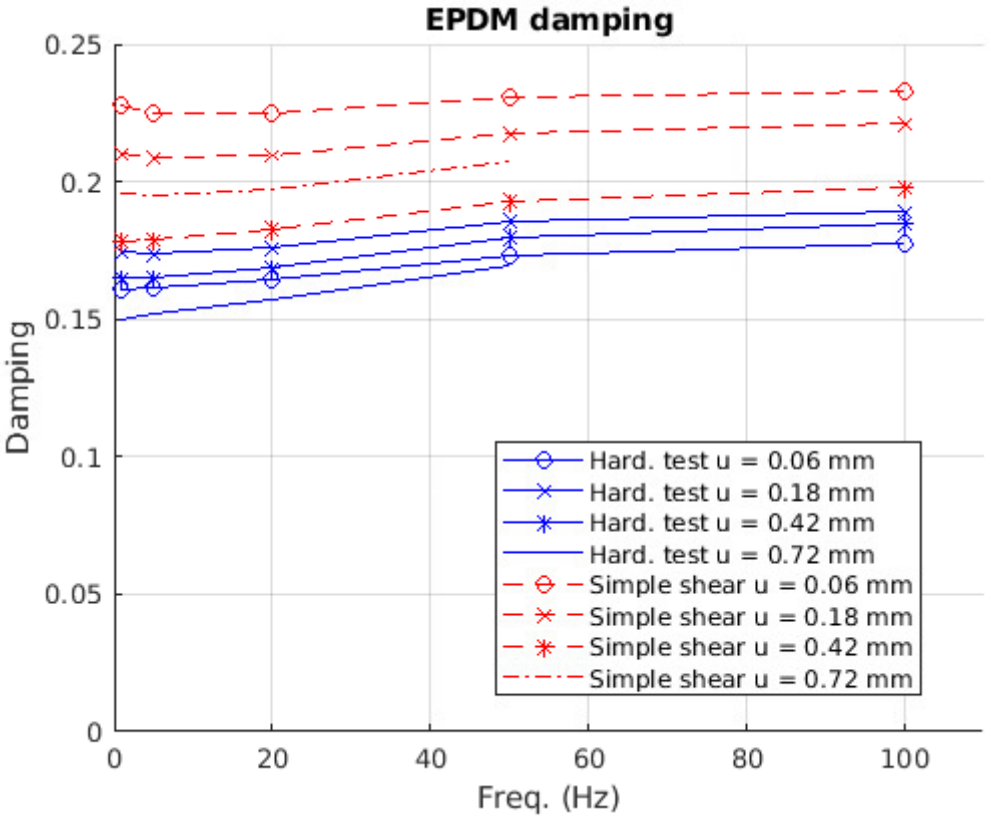
EPDM damping
Damping
Freq. (Hz)
0
0.05
0.1
0.15
0.2
0.25
0
20
40
60
80
100
Hard. test u = 0.06 mm
Hard. test u = 0.18 mm
Hard. test u = 0.42 mm
Hard. test u = 0.72 mm
Simple shear u = 0.06 mm
Simple shear u = 0.18 mm
Simple shear u = 0.42 mm
Simple shear u = 0.72 mm

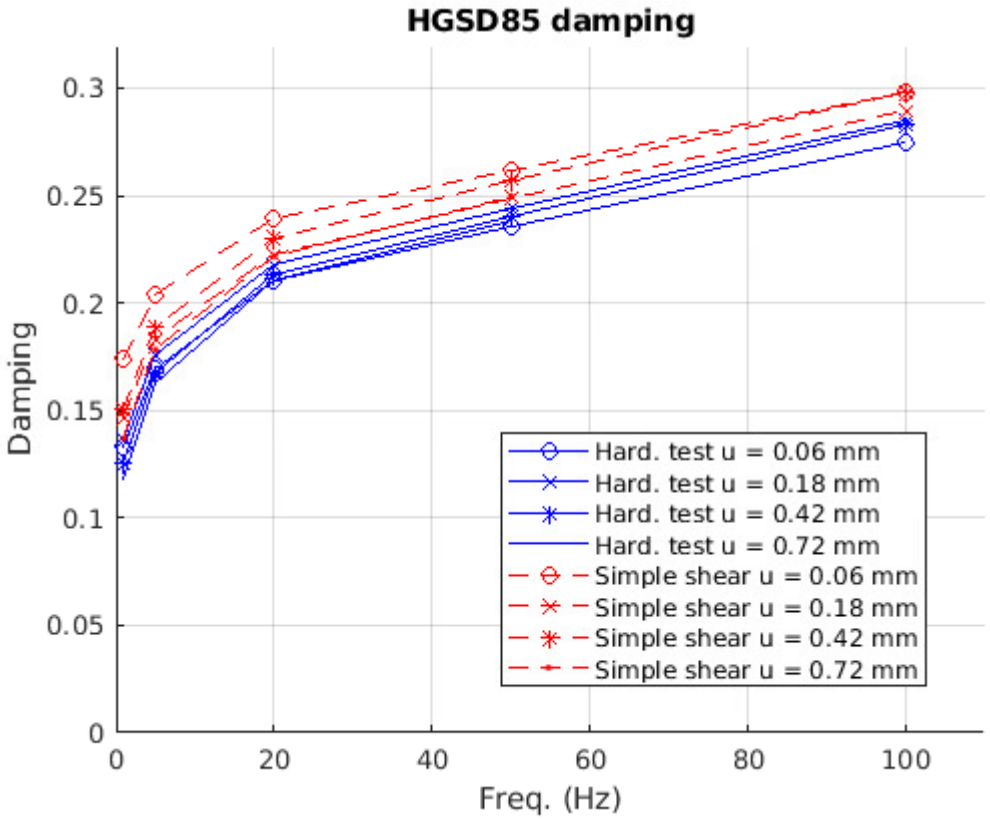

Figure 38. Damping from modified hardness test (solid blue lines) and from simple shear test (dashed red lines).

Just like for the dynamic shear modulus, the lines (blue solid lines and red dashed lines) seem to have the same shape, but they do not align to each other very well. A new set of amplitudes are tested for the simple shear test, and in Figure 39 the results can be viewed.

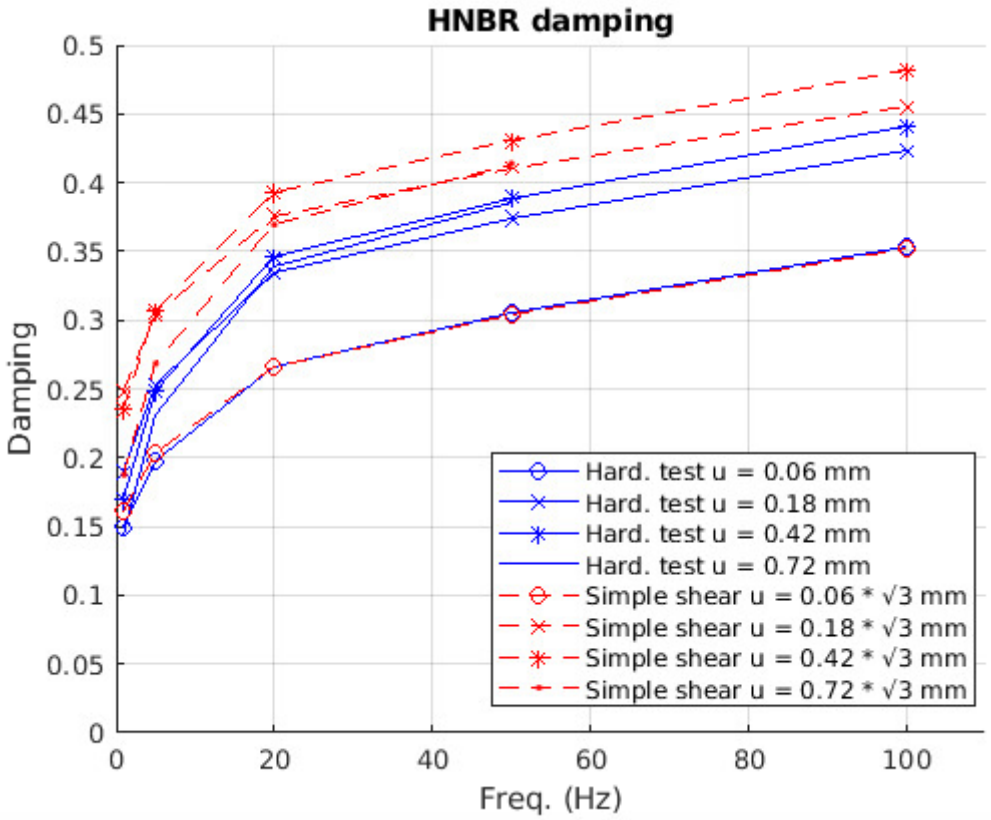
HNBR damping
Damping
Freq. (Hz)
0
0.05
0.1
0.15
0.2
0.25
0.3
0.35
0.4
0.45
0.5
0
20
40
60
80
100
Hard. test u = 0.06 mm
Hard. test u = 0.18 mm
Hard. test u = 0.42 mm
Hard. test u = 0.72 mm
Simple shear u = 0.06 * √3 mm
Simple shear u = 0.18 * √3 mm
Simple shear u = 0.42 * √3 mm
Simple shear u = 0.72 * √3 mm

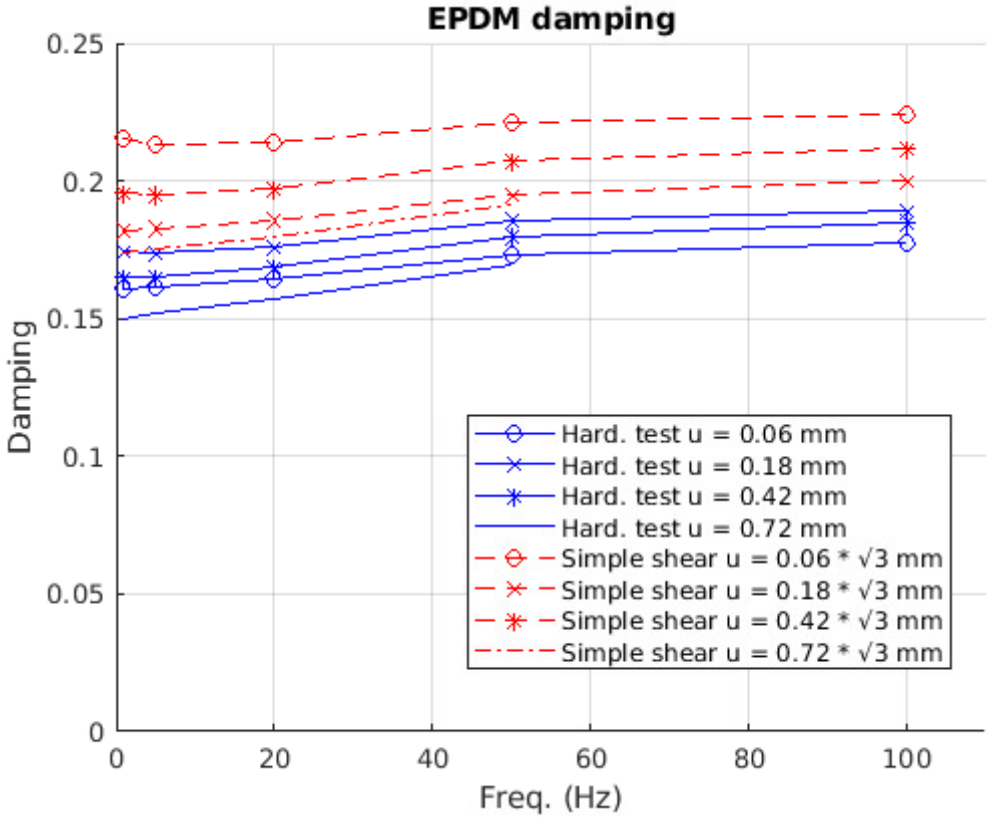
EPDM damping
Damping
Freq. (Hz)
0
0.05
0.1
0.15
0.2
0.25
0
20
40
60
80
100
Hard. test u = 0.06 mm
Hard. test u = 0.18 mm
Hard. test u = 0.42 mm
Hard. test u = 0.72 mm
Simple shear u = 0.06 * √3 mm
Simple shear u = 0.18 * √3 mm
Simple shear u = 0.42 * √3 mm
Simple shear u = 0.72 * √3 mm

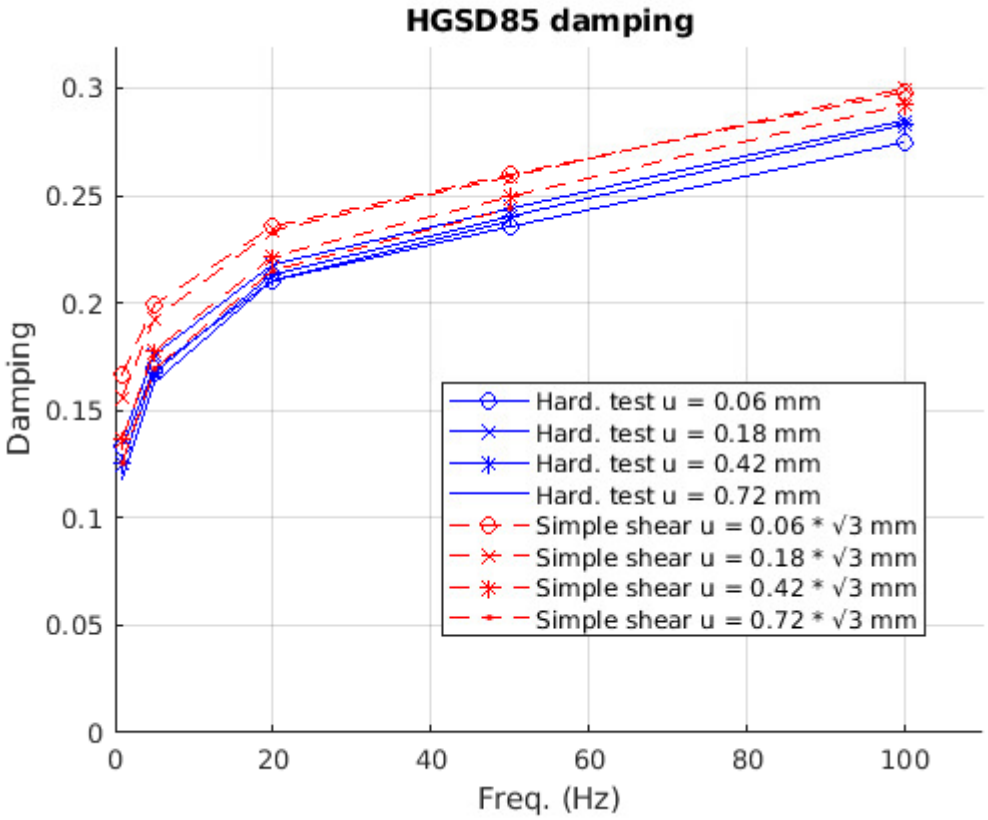

Figure 39. Damping from modified hardness test (solid blue lines) and from simple shear test (dashed red lines).

From Figure 39 above the damping for the modified hardness test seem to align more accurately to the damping for the simple shear test. However, there is still some difference in the damping values between the simple shear test and modified hardness test, which is most likely due to the amplitude not quite matching perfectly.

7 Conclusion and further work

By using the modified hardness test, it is proven that the use of energy balance equation works well for static characterization of elastomers, but not so well for the dynamic characterization. However, the alternative method which assume a direct connection between dynamic stiffness K_{dyn} and dynamic shear modulus G_{dyn} as $\alpha \cdot K_{dyn} = G_{dyn}$ proved to be a much better method when finding the equivalent dynamic shear modulus $G_{dyn}(\kappa_{eq}, f)$, since a single value alpha could be found for all frequencies and amplitudes independently of the material type.

Also, a relatively good connection between the indentation depth u and shear strain κ was found (when finding $G_{dyn}(\kappa_{eq}, f)$) by assuming pure compression for the modified hardness test and putting the first invariants of both compression and simple shear equal.

The damping for modified hardness test is calculated the same way as for the simple shear test, since the boundary condition should not affect the damping of the material. By looking at the results it is evident that the damping for modified hardness test has the same frequency dependence as for simple shear test. However, the amplitude dependence of damping for modified hardness test did not match the damping for simple shear, meaning that there probably is a better amplitude connection that could be found in order to obtain better results for the damping. But with an error that looks to be small the used amplitude connection is still a good approximation.

There is more work to be done when comparing the modified hardness test with simple shear test, and a few examples are listed below

- The amplitude connection between shear amplitude κ and indentation depth u could be investigated further. This could be done by assuming a linear connection between the modified hardness test amplitude and simple shear test amplitude as $u_{m.hard.test} = \beta \cdot u_{simpleShear}$ and doing a sweep of different β-values.

- The modified hardness test should be verified for both static and dynamic characterization by doing experimental tests with other rubber materials than those tested using finite element analysis.

- One could also investigate how different dimensions might affect the result for the modified hardness test (example: different radius and thickness of the rubber specimen, different indentation radius for the needle and different preload before the dynamic load is applied).

8 References

[1]
Woodford, Chris. (2008/2019) *Rubber*. Retrieved from: https://www.explainthatstuff.com/rubber.html [Accessed Mars 2019]

[2]
Synthetic rubber, From *Wikipedia.* Accessed Mars 2019. URL: https://en.wikipedia.org/wiki/Synthetic_rubber

[3]
Morton, M (1999), *Rubber Technology, Third Edition*, ISBN 978-90-481-4010-7

[4]
Yashoda (2016) *Difference Between Natural Rubber and Synthetic Rubber*. Retrieved from: http://pediaa.com/difference-between-natural-rubber-and-synthetic-rubber/ [Accessed Mars 2019]

[5]
Austrell, P-E (1997), *Modelling of elasticity and damping for filled elastomers*, Report TVSM-1009, Division of Structural Mechanics, Lund University

[6]
Rubber – History of Rubber, From *Soft Schools*. Accessed Mars 2019. URL: http://www.softschools.com/inventions/history/rubber_history/290/

[7]
Types of Synthetic Rubber, From *Industrial Rubber Goods*. Accessed Mars 2019. URL: http://www.industrialrubbergoods.com/types-of-synthetic-rubber.html

[8]
Olsson, A K. (2007), *Finite element procedures in modelling the dynamic properties of rubber*, Report TVSM-1021, Division of Structural Mechanics, Lund University

[9]
Carr, K.E. (2017) *What is rubber? History of rubber*. Quatr.us Study Guides, Retrieved from: https://quatr.us/science/rubber-history-rubber.htm [Accessed Mars 2019]

[10]
Ristinmaa, M. (2018), *Introduction to Non-linear Finite Element Method*, Course material for *FEM Nonlinear systems* (FHLN20), Division of Solid Mechanics, Lund University

[11]
Finite strain theory, From *Wikipedia.* Accessed April 2019. URL: https://en.wikipedia.org/wiki/Finite_strain_theory

[12]
Scott, J.R, (1948), *Improved method of expressing hardness of vulcanized rubber*, J. Rubb. Research 17, p. 145, 1948

[13]
Lindley, P.D, (1974), *Engineering Design with Natural Rubber*, MRPRA 1974

[14]
Rivlin, R.S., (1948), *Large elastic deformations of isotropic materials, IV. Further developments of the general theory.,* Phil. Trans. R. Soc. A241, pp. 379-397, 1948

[15]
Austrell, P.-E., Kallio 2 & Gutkin, R. (no date) *Static and dynamic characterization of elastomers for FE-simulations by a modified hardness test*, Structural Mechanics at Lund University & Volvo Car Cooperation in Gothenburg, Sweden (Unpublished paper).

[16]
ABAQUS Analysis User's Manual from **ABAQUS Version 6.6 Documentation Collection**. Can be obtained from following URL: https://classes.engineering.wustl.edu/2009/spring/mase5513/abaqus/docs/v6.6/books/usb/default.htm [Accessed April 2019]

[17]
Austrell, P.-E. (2019), Lecture notes from the course *Structural Dynamic Computing* (VSMN10), Accessed in May 2019 and can be obtained from: http://www.byggmek.lth.se/utbildning/kurser/vsmn10-strukturdynamiska-beraekningar/

[18]
Engineering ToolBox, (2009). *Densities of Solids*. [online] Available at: https://www.engineeringtoolbox.com/density-solids-d_1265.html [Accessed June 2019].

9 Appendix

The strain measures used when modelling large deformations are presented in this chapter. Also, the finite element method is briefly explained along with the different time stepping procedures used for dynamic calculations.

9.1 Strain measures

Considering a simple bar with constant cross-sectional area A_0 and initial length l_0. Load can only be applied through its centre end point resulting in homogenous deformation throughout the bar. After loading is applied the bar length changes to l, and the size of the new length depend on the size of the load. With this the stretch measure can be introduced [10]

$$\Lambda = \frac{l}{l_0}$$

With the stretch measure introduced the strain measure can be considered which is independent of rigid body motion and rotation. The strain can be determined by introducing a function that only depends on the stretch [10]

$$\varepsilon = f(\Lambda)$$

where it is required that $f(1) = 0$ which means that there is no strain when the length of the bar is kept unchanged, $df(1)/d\Lambda = 1$ which ensures that all choices of functions degenerates to the same infinitesimal strain tensor when the stretch is close to 1, and that $f(\Lambda)$ is a smooth monotonic function which ensures that there is a unique relation between the strain and the stretch. With this said a general format of the strain measures can be considered according to below [10]:

$$\varepsilon^{(m)} = \begin{cases} \frac{1}{m}(\Lambda^m - 1) & m \neq 0 \\ \ln(\Lambda) & m = 0 \end{cases}$$

And the most common strain measures used are listed below [10]:

$\varepsilon^{(-2)} = \frac{1}{2}(1 - \Lambda^{-2})$	Almansi's strain
$\varepsilon^{(-1)} = 1 - \Lambda^{-1}$	$(no\ name\ found\ in\ literature)$
$\varepsilon^{(0)} = \ln(\Lambda)$	Logarithmic strain or Hencky strain
$\varepsilon^{(1)} = \Lambda - 1$	Nominal strain or Biot strain
$\varepsilon^{(2)} = \frac{1}{2}(\Lambda^2 - 1)$	Lagrangian strain or Green's strain

Inserting the definition of the stretch in the strain measures yield a function that depends on the lengths, for instance the nominal strain and Green's strain [10]

$$\varepsilon_l = \Lambda - 1 = \frac{l - l_0}{l_0}$$

$$\varepsilon_g = \frac{1}{2}(\Lambda^2 - 1) = \frac{l^2 - l_0^2}{2l_0^2}$$

9.2 Strain energy

Considering an arbitrary geometry, there is energy stored in every point in the material which is released when the molecules rearrange themselves during deformation, introducing the strain energy. The increment in strain energy is defined as [10]

$$dw = \sigma \cdot d\varepsilon$$

where σ denotes the stress and $d\varepsilon$ denotes the incremental strain. When integrating the above equation from undeformed state to deformed state yields the total strain energy [10]

$$w = \int_0^{\varepsilon} \sigma(\varepsilon)\, d\varepsilon$$

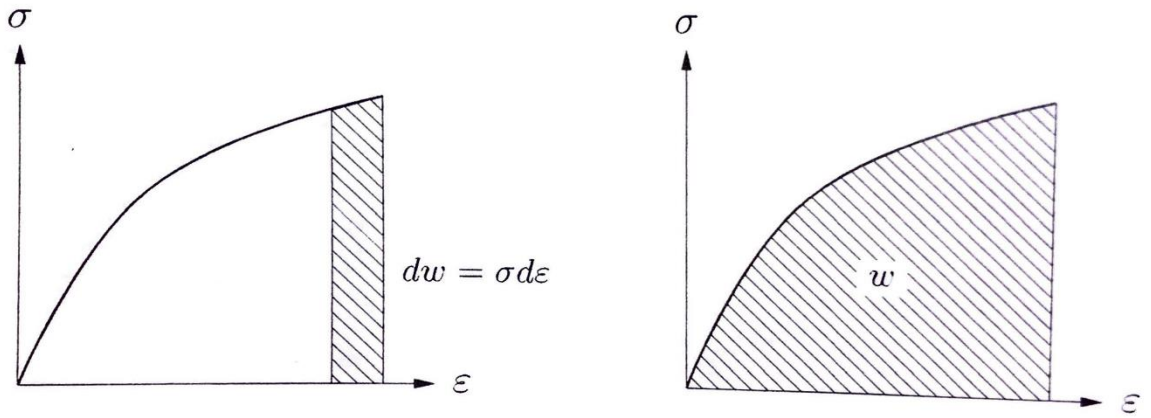

Figure 40. Incremental strain energy and strain energy for uniaxial loading. Source: [10]

Based on above there exist a potential function which is dependent on the strain [10]

$$w = w(\varepsilon)$$

and the stress strain relation is given by

$$\sigma = \frac{dw(\varepsilon)}{d\varepsilon}$$

If the stress-strain relation is derived from a strain energy function the material is called hyperelastic material [10].

Since there are different types of strain measures used when modelling non-linearity in materials, different types of energy conjugated stresses can be obtained [10], for example the nominal stress σ_l is obtained using nominal strain ε_l and Green's stress σ_g is obtained using Green's strain ε_g.

Although there exist different types of strains and stresses, the strain energy will always stay the same independent of the choice of strain measure according to following [10]

$$dw = \sigma_l \cdot d\varepsilon_l = \sigma_g \cdot d\varepsilon_g$$

From previous section it is noted that all strain measures can be written in the stretch quantity [10], which means that the strain energy function also can be rewritten as

$$w = w(\Lambda)$$

and with the nominal strain and Green's strain as examples one can derive the stresses according to the following [10]

$$\sigma_l = \frac{dw}{d\varepsilon_l} = \frac{dw}{d\Lambda}$$

and

$$\sigma_g = \frac{dw}{d\varepsilon_g} = \frac{dw}{d\Lambda}\frac{1}{\Lambda}$$

The stretch measure is commonly used when deriving strain energy functions for materials sustaining large deformations, i.e. elastomers.

9.3 Deformation gradient

Previously the stretch measure and strain measures has been introduced for a one-dimensional system. When modelling 2- or 3-dimensional systems, something called *deformation gradient* is used instead, which will be introduced in this chapter.

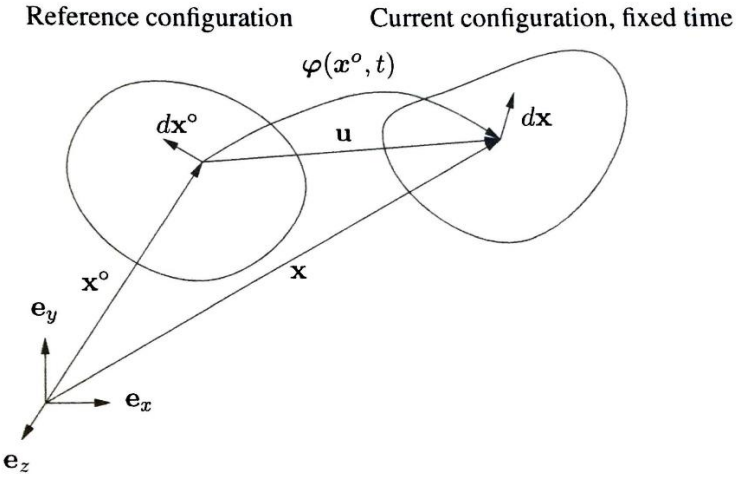

*Figure 41. Displacement **u** from reference configuration $\mathbf{x}^0$ to current configuration **x** at fixed time. Source: [10]*

In Figure 41 above we have an arbitrary system in its undeformed configuration, denoted as *reference configuration*. Each point in the reference configuration is identified by its material coordinates $\boldsymbol{x^o} = (x^o, y^o, z^o)$ or $\boldsymbol{x^o} = (x_1^o, x_2^o, x_3^o)$. After the reference configuration has been deformed it will enter the deformed configuration, denoted as *current configuration* in Figure 41. Each point in the deformed configuration

are now identified by its new material coordinates $\boldsymbol{x} = (x, y, z)$ or $\boldsymbol{x} = (x_1, x_2, x_3)$.The flow/movement over time of all particles in the system can be described with a flow-equation $\boldsymbol{\varphi}(\boldsymbol{x^o}, t)$. At initial time (t = 0) the flow is equal to the initial coordinates, e.g. $\boldsymbol{\varphi}(\boldsymbol{x^o}, 0) = \boldsymbol{x^o}$. With this said, a function of the new material coordinates at a fixed time t can be described with the following relation [10]

$$\boldsymbol{x}(\boldsymbol{x^o}, t) = \boldsymbol{\varphi}(\boldsymbol{x^o}, t) = \boldsymbol{x^o} + \boldsymbol{u}(\boldsymbol{x^o}, t) \tag{9.1}$$

Where $\boldsymbol{u}(\boldsymbol{x^0}, t)$ is the displacement vector. Let's consider the change in distance between two particles close to each other. The distance in the undeformed configuration is denoted $d\boldsymbol{x^0}$ and the same distance in the deformed configuration is denoted $d\boldsymbol{x}$. Since $\boldsymbol{x} = \boldsymbol{x}(\boldsymbol{x^0}, t)$ it follows that $d\boldsymbol{x}$ can be rewritten as [10]

$$d\boldsymbol{x} = \boldsymbol{F} \cdot d\boldsymbol{x^o} \tag{9.2}$$

Where

$$\boldsymbol{F} = \boldsymbol{\nabla_o x}$$

$\boldsymbol{F}$ is defined as the *deformation gradient* and is sometimes also called *deformation tensor* or *deformation matrix*. The deformation gradient is a square and invertible matrix, and can be written in tensor notation as [10]

$$\boldsymbol{F} = F_{ij} = \frac{\partial x_i}{\partial x_j^o}$$

Tensor notation is a general way of describing vectors and matrices, for instance the material coordinates in deformed configuration can be denoted in tensor notation as $[\boldsymbol{x}] = [x_i]$ where i is a number from 1 to 3. The deformation gradient is written in matrix format according to following [10]:

$$\boldsymbol{F} = [\mathbf{F}] = \left[\frac{\partial x_i}{\partial x_j^o}\right] = \begin{bmatrix} \frac{\partial x}{\partial x^o} & \frac{\partial x}{\partial y^o} & \frac{\partial x}{\partial z^o} \\ \frac{\partial y}{\partial x^o} & \frac{\partial y}{\partial y^o} & \frac{\partial y}{\partial z^o} \\ \frac{\partial z}{\partial x^o} & \frac{\partial z}{\partial y^o} & \frac{\partial z}{\partial z^o} \end{bmatrix}$$

Where

$$[x_i] = (x_1, x_2, x_3) = (x, y, z)$$
$$\left[x_j^o\right] = (x_1^o, x_2^o, x_3^o) = (x^o, y^o, z^o)$$

Moreover, returning to equation (9.1) it is found that the change in distance can be written as follows [10]:

$$d\boldsymbol{x} = d\boldsymbol{x^o} + \boldsymbol{\nabla_o u} \cdot d\boldsymbol{x^o} = (\boldsymbol{I} + \boldsymbol{\nabla_o u}) \cdot d\boldsymbol{x^o}$$

And comparing with equation (9.2) one can conclude that the following holds [10]

$$\boldsymbol{F} = \boldsymbol{I} + \boldsymbol{\nabla_o u}$$

Where $\boldsymbol{I}$ is the unit matrix and $\boldsymbol{\nabla_o u}$ is the *displacement gradient* and is defined as [10]

$$[\boldsymbol{\nabla_o u}] = \left[\frac{\partial u_i}{\partial x_j^o}\right] = \begin{bmatrix} \frac{\partial u_x}{\partial x^o} & \frac{\partial u_x}{\partial y^o} & \frac{\partial u_x}{\partial z^o} \\ \frac{\partial u_y}{\partial x^o} & \frac{\partial u_y}{\partial y^o} & \frac{\partial u_y}{\partial z^o} \\ \frac{\partial u_z}{\partial x^o} & \frac{\partial u_z}{\partial y^o} & \frac{\partial u_z}{\partial z^o} \end{bmatrix}$$

With the deformation gradient introduced the deformation of a body can be determined where distances will be considered. Considering the distances between two particles, the length of vector $\boldsymbol{dx^o}$ can be denoted by $\boldsymbol{dl^o}$ and the length of vector $\boldsymbol{dx}$ can be denoted by $\boldsymbol{dl}$. The following is then obtained [10]

$$\boldsymbol{dl^{o\,2} = dx^o \cdot dx^o}$$
$$\boldsymbol{dl^2 = dx \cdot dx}$$

Taking advantage of (9.2) we have

$$\boldsymbol{dl^2 = dx^o \cdot F^T \cdot F \cdot dx^o}$$

Using the definition for Green's strain the deformation can be written

$$\boldsymbol{\frac{dl^2 - dl^{o\,2}}{2dl^{o\,2}} = n^o \cdot E \cdot n^o}$$

Where $\boldsymbol{n^o}$ is a constant unit vector, which makes it evident that the deformation is characterized by $\boldsymbol{E}$, also called *Green's strain tensor* [10]. This tensor is defined as

$$\boldsymbol{E = \frac{1}{2}(C - I) = \frac{1}{2}(F^T \cdot F - I)}$$

Where $\boldsymbol{C}$ is the *right Cauchy-Green's deformation tensor*. Reversing the order of the multiplication one can obtain the *left Cauhy-Green deformation tensor* and is defined as [11]

$$\boldsymbol{B = F \cdot F^T}$$

These deformation tensors are usually used to describe stress-strain laws for materials that can sustain large deformation in two- or three-dimensional models, because they have shown to be independent of pure rotation of a body. Below follows a brief explanation of how pure rotation is cancelled out in the left and right Cauchy Green's deformation tensors.

9.3.1 Polar decomposition

With the deformation gradient $\boldsymbol{F}$ being a square and invertible matrix, it can be decomposed into a product of two matrices using polar decomposition, one being an orthogonal tensor and the other being a positive definite symmetric tensor [11]:

$$\boldsymbol{F} = \boldsymbol{R} \cdot \boldsymbol{U} = \boldsymbol{V} \cdot \boldsymbol{R}$$

Where $\boldsymbol{R}$ is the orthogonal tensor, i.e. $\boldsymbol{R}^{-1} = \boldsymbol{R}^{T}$ and $det\boldsymbol{R} = +1$, representing the rotation, and $\boldsymbol{U}$ and $\boldsymbol{V}$ being the positive definite symmetric tensors, i.e. $\boldsymbol{x} \cdot \boldsymbol{U} \cdot \boldsymbol{x} \geq 0$ and $\boldsymbol{x} \cdot \boldsymbol{V} \cdot \boldsymbol{x} \geq 0$, representing the right ($\boldsymbol{U}$) and left ($\boldsymbol{V}$) stretch tensors [11].

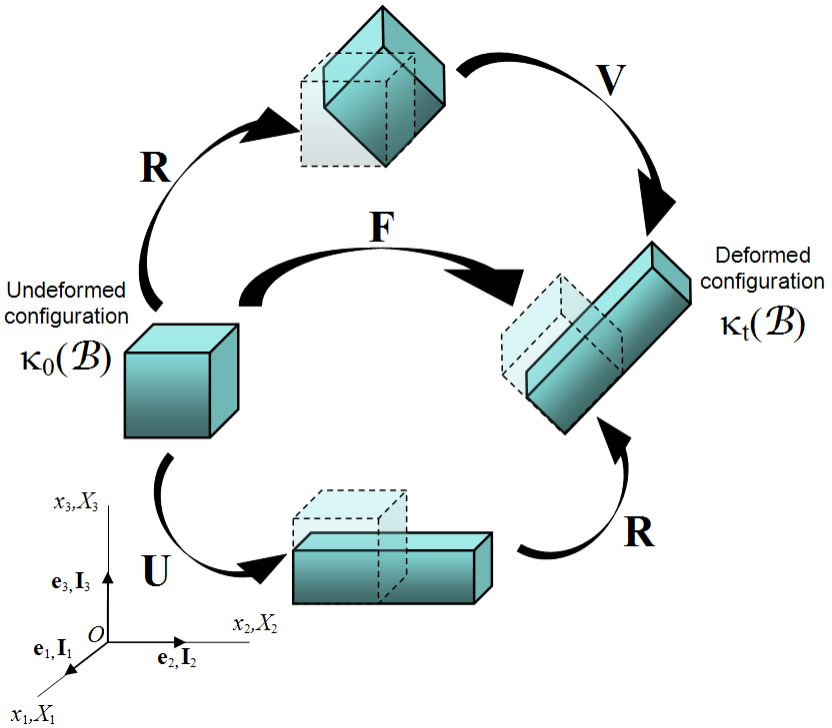

Figure 42. Polar decomposition presented graphicly. Source: [11]

Because of the orthogonality of $\boldsymbol{R}$ it follows that [10]

$$\boldsymbol{R} \cdot \boldsymbol{R}^{T} = \boldsymbol{I}$$

Therefore, when using Green's strain as the strain measure results in a cancelation of the translation term, leaving only the deformation term in the strain tensor as

$$\boldsymbol{C} = \boldsymbol{F}^{\boldsymbol{T}}\boldsymbol{F} = \boldsymbol{U}^{\boldsymbol{T}}\boldsymbol{U} \qquad \boldsymbol{or} \qquad \boldsymbol{B} = \boldsymbol{F}\boldsymbol{F}^{\boldsymbol{T}} = \boldsymbol{V}\boldsymbol{V}^{\boldsymbol{T}}$$

9.4 Finite Element Method

Here the derivation of the finite element method is briefly explained along with the different time stepping procedures used for dynamic calculations.

9.4.1 Equation of motion

Consider a three-dimensional body loaded by a body force $\boldsymbol{b}(\boldsymbol{x},t)$ and a traction force $\boldsymbol{t}(\boldsymbol{x},t)$ [17].

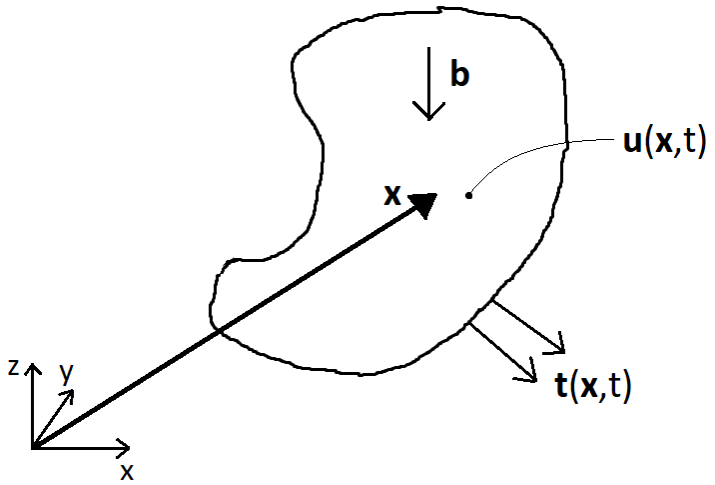

Figure 43. Arbitrary body with body force and surface traction force.

The loading causes displacements $\boldsymbol{u}(\boldsymbol{x},t)$ and stresses $\boldsymbol{\sigma}(\boldsymbol{x},t)$ in the body. The equilibrium equation according to Newton's second law can be written as [17]

$$\widetilde{\boldsymbol{\nabla}}\boldsymbol{\sigma} + \boldsymbol{b} = \rho\ddot{\boldsymbol{u}}$$

Where

$$\widetilde{\boldsymbol{\nabla}} = \begin{bmatrix} \frac{\partial}{\partial x} & 0 & 0 & \frac{\partial}{\partial y} & \frac{\partial}{\partial z} & 0 \\ 0 & \frac{\partial}{\partial y} & 0 & \frac{\partial}{\partial x} & 0 & \frac{\partial}{\partial z} \\ 0 & 0 & \frac{\partial}{\partial z} & 0 & \frac{\partial}{\partial x} & \frac{\partial}{\partial y} \end{bmatrix};\ \boldsymbol{\sigma} = \begin{bmatrix} \sigma_{xx} \\ \sigma_{yy} \\ \sigma_{zz} \\ \sigma_{xy} \\ \sigma_{xz} \\ \sigma_{yz} \end{bmatrix};\ \boldsymbol{b} = \begin{bmatrix} b_x \\ b_y \\ b_z \end{bmatrix}$$

The equation above is known as *the strong form of the equilibrium equation*. Deriving the FE-formulation used in the FE-codes the strong form must be rewritten into the weak form first [17].

Starting off by multiplying with a time-independent weight vector $\boldsymbol{w}(\boldsymbol{x})$ and integrating over the volume of the body [17]

$$\int_V \boldsymbol{w}^T\widetilde{\boldsymbol{\nabla}}\boldsymbol{\sigma}\, dV + \int_V \boldsymbol{w}^T\boldsymbol{b}\, dV = \int_V \boldsymbol{w}^T\rho\ddot{\boldsymbol{u}}\, dV$$

The first term in the equation above can be rewritten using Gauss divergence theorem [17]

$$\int_V \boldsymbol{w}^T \tilde{\boldsymbol{\nabla}} \boldsymbol{\sigma}\, dV = \int_S \boldsymbol{w}^T \boldsymbol{t}\, dS - \int_V \left(\tilde{\boldsymbol{\nabla}} \boldsymbol{w}\right)^T \boldsymbol{\sigma}\, dV$$

Where $\boldsymbol{t} = \boldsymbol{S}^T \boldsymbol{n}$, $\boldsymbol{S}$ being the stress tensor and $\boldsymbol{n}$ being the unit vector.

Yielding the weak formulation of the equilibrium equation

$$\int_S \boldsymbol{w}^T \boldsymbol{t}\, dS + \int_V \boldsymbol{w}^T \boldsymbol{b}\, dV = \int_V \boldsymbol{w}^T \rho \ddot{\boldsymbol{u}}\, dV + \int_V \left(\tilde{\boldsymbol{\nabla}} \boldsymbol{w}\right)^T \boldsymbol{\sigma}\, dV$$

FE-approximation can now be introduced and included in the weak form by adopting the Galerkin method [17]

$$\begin{cases} \boldsymbol{w} = \boldsymbol{N} \cdot \boldsymbol{c} \\ \boldsymbol{u} = \boldsymbol{N} \cdot \boldsymbol{a} \\ \ddot{\boldsymbol{u}} = \boldsymbol{N} \cdot \ddot{\boldsymbol{a}} \\ \tilde{\boldsymbol{\nabla}} \boldsymbol{N} = \boldsymbol{B} \end{cases}$$

Where $\boldsymbol{N}$ are the shape functions, $\boldsymbol{c}$ being an arbitrary constant vector, $\boldsymbol{a}$ is the nodal displacement vector and $\ddot{\boldsymbol{a}}$ is the nodal acceleration vector. The weak formulation is rewritten according to following [17]

$$\boldsymbol{c}^T \int_S \boldsymbol{N}^T \boldsymbol{t}\, dS + \boldsymbol{c}^T \int_V \boldsymbol{N}^T \boldsymbol{b}\, dV = \boldsymbol{c}^T \int_V \boldsymbol{N}^T \rho \boldsymbol{N}\, dV \cdot \ddot{\boldsymbol{a}} + \boldsymbol{c}^T \int_V \boldsymbol{B}^T \boldsymbol{\sigma}\, dV$$

Since $\boldsymbol{c}$ is arbitrary it can be cancelled out. Also, all the terms on the left side of the equal sign describe the applied forces and reaction forces on the body, why they can be simplified into the force vector $\boldsymbol{f} = \int_S \boldsymbol{N}^T \boldsymbol{t}\, dS + \int_V \boldsymbol{N}^T \boldsymbol{b}\, dV$. The mass matrix is also introduced as $\boldsymbol{M} = \int_V \boldsymbol{N}^T \rho \boldsymbol{N}\, dV$, and finally the FE-formulation (without damping) used for dynamic calculations can be written [17]

$$\boldsymbol{f} = \boldsymbol{M}\ddot{\boldsymbol{a}} + \int_V \boldsymbol{B}^T \boldsymbol{\sigma}\, dV$$

For static calculations the equation above can be reduced to

$$\boldsymbol{f} = \int_V \boldsymbol{B}^T \boldsymbol{\sigma}\, dV$$

This formulation is valid for all constitutive relations $\boldsymbol{\sigma}$. The term on the right side of the equation above can be reduced to $\int_V \boldsymbol{B}^T \boldsymbol{\sigma}\, dV = \boldsymbol{K}\boldsymbol{a}$ with some manipulations done, where **K** is the stiffness matrix and **a** is the displacement vector. For static calculation, if the geometry or material is non-linear the stiffness matrix will change when load is applied and the geometry is deformed making it dependent on the displacement vector **a**, why it is required that an incremental load or displacement procedure is adopted.

This is not the case for a linear material model and geometry. For dynamic situations it is usually required that an incremental time-stepping procedure is adopted.

9.4.2 Time-stepping procedure

When doing dynamic FE-calculations a time stepping procedure has to be implemented with initial conditions such as initial displacement and acceleration. There are two different types of time stepping procedures used in today's FE applications: explicit method and implicit method [17].

For **implicit** calculations the equation of motion is solved by finding the displacement vector $\boldsymbol{a}$ in the current time step (n) first and then calculating the rest of the unknown quantities by using the information that is already known in previous time step (n-1). This method is also known as the *Newmark iteration scheme* which uses Newton-Raphson iterations in order to enforce equilibrium of external and internal forces before moving forward to the next time increment, making it both an iterative and incremental algorithm. The advantage with this method is that the scheme is relatively stable for large time steps making it unconditionally stable. The advantage with this is that large timesteps can be used if smaller time steps won't make the results more accurate. The disadvantage however is that since the displacement vector $\boldsymbol{a}$ is solved directly it is required that the inverse of the stiffness matrix $\mathbf{K}$ is calculated, which is a very expensive calculation since the stiffness matrix can be very complex. This is especially valid for nonlinear geometries and material models; the stiffness matrix must be updated after every increment since it is dependent on the displacement vector $\boldsymbol{a}$ [17].

For **explicit** calculations, instead of solving the equation of motion for displacement vector $\boldsymbol{a}$ it is instead solved for the acceleration vector $\ddot{\boldsymbol{a}}$. This is very advantageous since the inverse of the stiffness matrix is avoided and only the mass matrix must be inverted, which is less expensive when it comes to calculation costs. Also, since lower order elements are usually used for explicit calculations the mass matrix is lumped, meaning that it is a diagonal matrix and therefore makes the calculation of the inverse much faster. However, since Newton-Raphson iterations aren't done for explicit calculations (explicit scheme is only incremental) it is conditionally stable, meaning that very small time-steps, sometimes extremely small time-steps, must be used for accurate results [17].